



Limits on the Higgs boson lifetime and width from its decay to four charged leptons

The CMS Collaboration*

Abstract

Constraints on the lifetime and width of the Higgs boson are obtained from $H \rightarrow ZZ \rightarrow 4l$ events using data recorded by the CMS experiment during the LHC run 1 with an integrated luminosity of 5.1 and 19.7 fb^{-1} at a center-of-mass energy of 7 and 8 TeV, respectively. The measurement of the Higgs boson lifetime is derived from its flight distance in the CMS detector with an upper bound of $\tau_H < 1.9 \times 10^{-13} \text{ s}$ at the 95% confidence level (CL), corresponding to a lower bound on the width of $\Gamma_H > 3.5 \times 10^{-9} \text{ MeV}$. The measurement of the width is obtained from an off-shell production technique, generalized to include anomalous couplings of the Higgs boson to two electroweak bosons. From this measurement, a joint constraint is set on the Higgs boson width and a parameter $f_{\Lambda Q}$ that expresses an anomalous coupling contribution as an on-shell cross-section fraction. The limit on the Higgs boson width is $\Gamma_H < 46 \text{ MeV}$ with $f_{\Lambda Q}$ unconstrained and $\Gamma_H < 26 \text{ MeV}$ for $f_{\Lambda Q} = 0$ at the 95% CL. The constraint $f_{\Lambda Q} < 3.8 \times 10^{-3}$ at the 95% CL is obtained for the expected standard model Higgs boson width.

Submitted to Physical Review D

1 Introduction

The discovery of a new boson with mass of about 125 GeV by the ATLAS and CMS experiments [1–3] at the CERN LHC provides support for the standard model (SM) mechanism with a field responsible for generating the masses of elementary particles [4–9]. This new particle is believed to be a Higgs boson (H), the scalar particle appearing as an excitation of this field. The measurement of its properties, such as the lifetime, width, and structure of its couplings to the known SM particles, is of high priority to determine its nature.

The CMS and ATLAS experiments have set constraints of $\Gamma_H < 22 \text{ MeV}$ at 95% confidence level (CL) on the H boson total width [10, 11] from the ratio of off-shell to on-shell production. The precision on Γ_H from direct on-shell measurements alone is approximately 1 GeV [12, 13], which is significantly larger. The two experiments have also set constraints on the spin-parity properties and anomalous couplings of the H boson [14–18], finding its quantum numbers to be consistent with $J^{PC} = 0^{++}$ but allowing small anomalous coupling contributions. No direct experimental limit on the H boson lifetime was set, and the possible presence of anomalous couplings was not considered in the constraints on the H boson width. This paper provides these two measurements.

The measurement of the H boson lifetime in this paper is derived from its flight distance in the CMS detector [19], and the measurement of the width is obtained from the off-shell production technique, generalized to include anomalous couplings of the H boson to two electroweak bosons, WW and ZZ . From the latter measurement, a joint constraint is set on the H boson width and a parameter that quantifies an anomalous coupling contribution as on-shell cross-section fraction. The event reconstruction and analysis techniques rely on the previously published results [10, 16, 17, 20], and their implementations are discussed in detail. Only the final state with four charged leptons is considered in this paper, but the constraints on the width could be improved by including final states with neutrinos in the off-shell production [10, 11]. Indirect constraints on the H boson width and lifetime are also possible through the combination of data on H boson production and decay rates [12, 21]. While such a combination tests the compatibility of the data with the SM H boson, it relies on stronger theoretical assumptions such as SM-like coupling ratios among the different final states.

Section 2 in this paper discusses the analysis methods for measuring the H boson lifetime, and for relating the anomalous couplings of the H boson to the measurement of Γ_H through the off-shell production technique. Section 3 discusses the CMS detector and event simulation, and Sec. 4 defines the selection criteria used in the analysis. Section 5 describes the analysis observables, categorization, and any related uncertainty. Section 6 provides the constraints on the H boson lifetime, while Sec. 7 provides the upper limits for both the H boson width and the anomalous coupling parameter investigated in this paper. The summary of results is provided in Sec. 8.

2 Analysis techniques

The lifetime of each H boson candidate in its rest frame is determined in a four-lepton event as

$$\Delta t = \frac{m_{4\ell}}{p_T} (\Delta \vec{r}_T \cdot \hat{p}_T), \quad (1)$$

where $m_{4\ell}$ is the four-lepton invariant mass, $\Delta \vec{r}_T$ is the displacement vector between the decay vertex and the production vertex of the H boson in the plane transverse to the beam axis, and \hat{p}_T and p_T are respectively the unit vector and the magnitude of the H boson transverse

momentum. The average Δt is inversely proportional to the total width:

$$\langle \Delta t \rangle = \tau_H = \frac{\hbar}{\Gamma_H} \quad (2)$$

The distribution of the measured lifetime Δt is used to set an upper limit on the average lifetime of the H boson, or equivalently a lower limit on its width Γ_H , and it follows the exponential distribution if known perfectly. The expected SM H boson average lifetime is $\tau_H \approx 48 \text{ fm}/c$ ($16 \times 10^{-8} \text{ fs}$) and is beyond instrumental precision. The technique summarized in Eq. (1) nonetheless allows the first direct experimental constraint on τ_H .

The upper bound on Γ_H is set using the off-shell production method [22–24] and follows the technique developed by CMS [10], where the gluon fusion and weak vector boson fusion (VBF) production mechanisms were considered in the analysis. The technique considers the H boson production relationship between the on-shell ($105.6 < m_{4\ell} < 140.6 \text{ GeV}$) and off-shell ($220 < m_{4\ell} < 1600 \text{ GeV}$) regions. Denoting each production mechanism with $\text{vv} \rightarrow \text{H} \rightarrow \text{ZZ}$ for H boson coupling to either strong ($\text{vv} = \text{gg}$) or weak ($\text{vv} = \text{VV}$) vector bosons vv , the on-shell and off-shell yields are related by

$$\sigma_{\text{vv} \rightarrow \text{H} \rightarrow \text{ZZ}}^{\text{on-shell}} \propto \mu_{\text{vvH}} \text{ and } \sigma_{\text{vv} \rightarrow \text{H} \rightarrow \text{ZZ}}^{\text{off-shell}} \propto \mu_{\text{vvH}} \Gamma_H, \quad (3)$$

where μ_{vvH} is the on-shell signal strength, the ratio of the observed and expected on-shell production cross sections for the four-lepton final state, which is denoted by either μ_{ggH} for gluon fusion production or μ_{VVH} for VBF production. The $\text{t}\bar{\text{t}}\text{H}$ process is driven by the H boson couplings to heavy quarks like the gluon fusion process, and the VH process by the H boson couplings to weak vector bosons like the VBF process. They are therefore parametrized with the same on-shell signal strengths μ_{ggH} and μ_{VVH} , respectively. The effects of signal-background interference are not shown in Eq. (3) for illustration but are taken into account in the analysis.

The relationship in Eq. (3) implies variations of the vvH couplings as a function of $m_{4\ell}$. This variation is assumed to be as in the SM in the gluon fusion process. The assumption is valid as long as the production is dominated by the top-quark loop and no new particles contribute to this loop. Variation of the HVV couplings, either in the VBF or VH production or in the $\text{H} \rightarrow \text{ZZ}$ decay, may depend on anomalous coupling contributions. An enhancement of the off-shell signal production is suggested with anomalous HVV couplings [10, 25–27], but neither experimental studies of off-shell production nor realistic treatment of signal-background interference has been done with these anomalous couplings. We extend the methodology of the recent analysis of anomalous HVV couplings of the H boson [17] to study these couplings and introduce in the scattering amplitude an additional term that depends on the H boson invariant mass, $(q_{V1} + q_{V2})^2$:

$$A(\text{HVV}) \propto \left[a_1 - e^{i\phi_{\Lambda_Q}} \frac{(q_{V1} + q_{V2})^2}{(\Lambda_Q)^2} - e^{i\phi_{\Lambda_1}} \frac{(q_{V1}^2 + q_{V2}^2)}{(\Lambda_1)^2} \right] m_V^2 \epsilon_{V1}^* \epsilon_{V2}^* + a_2 f_{\mu\nu}^{*(1)} f^{*(2),\mu\nu} + a_3 f_{\mu\nu}^{*(1)} \tilde{f}^{*(2),\mu\nu}, \quad (4)$$

where $f^{(i)\mu\nu} = \epsilon_{V_i}^\mu q_{V_i}^\nu - \epsilon_{V_i}^\nu q_{V_i}^\mu$ is the field strength tensor of a gauge boson with momentum q_{V_i} and polarization vector ϵ_{V_i} , $\tilde{f}_{\mu\nu}^{(i)} = \frac{1}{2} \epsilon_{\mu\nu\rho\sigma} f^{(i),\rho\sigma}$ is the dual field strength tensor, the superscript $*$ designates a complex conjugate, and m_V is the pole mass of a vector boson. The a_i are complex coefficients, and the Λ_1 or Λ_Q may be interpreted as the scales of beyond-the-SM (BSM) physics. The complex phase of the Λ_1 and Λ_Q terms are explicitly given as ϕ_{Λ_1} and ϕ_{Λ_Q} , respectively. Equation (4) describes all anomalous contributions up to dimension five operators. In the SM,

only the a_1 term appears at tree level in couplings to ZZ and WW, and it remains dominant after loop corrections. Constraints on the anomalous contributions from the a_2 , a_3 and Λ_1 terms to the $H \rightarrow VV$ decay have been set by the CMS and ATLAS experiments [16–18] through on-shell H boson production.

The Λ_Q term depends only on the invariant mass of the H boson, so its contribution is not distinguishable from the SM in the on-shell region. This paper tests the Λ_Q term through the off-shell region. Equation (4) describes both ZZ and WW couplings, and it is assumed that Λ_Q is the same for both. The ratio of any loop contribution from a heavy particle in the HVV scattering amplitude to the SM tree-level a_1 term would be predominantly real, and the imaginary part of the ratio would be small. If the contribution instead comes from an additional term to the SM Lagrangian itself, this ratio can only be real. Therefore, only real coupling ratios are tested such that $\cos \phi_{\Lambda Q} = \pm 1$ and $a_1 \geq 0$, where $a_1 = 2$ and $\Lambda_Q \rightarrow \infty$ correspond to the tree-level SM HVV scattering with $\mu_{ggH} = \mu_{V VH} = 1$. The effective cross-section fraction due to the Λ_Q term, denoted as $f_{\Lambda Q}$, allows a parametrization similar to the conventions of Λ_1 in Ref. [17]. It is defined for the on-shell $gg \rightarrow H \rightarrow VV$ process assuming no contribution from other anomalous couplings as

$$f_{\Lambda Q} = \frac{m_H^4 / \Lambda_Q^4}{|a_1|^2 + m_H^4 / \Lambda_Q^4}. \quad (5)$$

The HVV couplings in Eq. (4) appear in both production and decay for the VBF and VH mechanisms while they appear only in decay for H boson production through gluon fusion. Isolating the former two production mechanisms, therefore, enhances the sensitivity to the contribution of anomalous couplings. While the previous study of the H boson width [10] employs dijet tagging only in the on-shell region, VBF jet identification is also extended to the off-shell region in this analysis with techniques from Ref. [20]. A joint constraint is obtained on Γ_H , $f_{\Lambda Q}$, μ_{ggH} , and $\mu_{V VH}$, where the latter two parameters correspond to the H production strength in gluon fusion, and VBF or VH production mechanisms in the on-shell region, respectively.

3 The CMS experiment and simulation

The CMS detector, described in detail in Ref. [19], provides excellent resolution for the measurement of electron and muon momenta and impact parameters near the LHC beam interaction region. Within the superconducting solenoid (3.8 T) volume of CMS, there are a silicon pixel and strip tracker, a lead tungstate crystal electromagnetic calorimeter (ECAL) and a brass and scintillator hadron calorimeter. Muons are identified in gas-ionization detectors embedded in the iron flux return placed outside the solenoid. The data samples used in this analysis are the same as those described in Refs. [10, 16, 17, 20], corresponding to an integrated luminosity of 5.1 fb^{-1} collected in proton-proton collisions at LHC with center-of-mass energy of 7 TeV in 2011 and 19.7 fb^{-1} at 8 TeV in 2012. The uncertainties in the integrated luminosity measurement are 2.2% and 2.6% for the 2011 and 2012 data sets, respectively [28, 29].

The H boson signal production through gluon fusion or in association with two fermions from either vector boson fusion or associated vector boson production may interfere with the background 4ℓ production with the same initial and final states. The background 4ℓ production is considered to be any process that does not include a contribution from the H boson signal. The on-shell Monte Carlo (MC) simulation does not require interference with the background because of the relatively small H boson width [10]. The off-shell production leads to a broad $m_{4\ell}$ spectrum and is generated using the full treatment of the interference between the signal and background for each production mechanism. Therefore, different techniques and tools

have been used for on-shell and off-shell simulation. The simulation of the H boson signal is performed at the measured value of the H boson pole mass $m_H = 125.6 \text{ GeV}$ in the 4ℓ final state [16], and the expected SM H boson width $\Gamma_H^{\text{SM}} = 4.15 \text{ MeV}$ [30, 31] along with several other Γ_H reference values.

The two dominant H boson production mechanisms, gluon fusion and VBF, are generated on-shell at next-to-leading order (NLO) in perturbative quantum chromodynamics (QCD) using the POWHEG [32–34] event generator. The decay of the H boson via $H \rightarrow ZZ \rightarrow 4\ell$, including interference effects of identical leptons in the final state and nonzero lifetime of the H boson, is modeled with JHUGEN 4.8.1 [35–37]. In addition, gluon fusion production with up to two jets at NLO in QCD has been generated using POWHEG with the HJJ program [38], where the MINLO procedure [39] is used to resum all large logarithms associated with the presence of a scale for merging the matrix element and the parton shower contributions. In all of the above cases, simulations with a wide range of masses m_H up to 1000 GeV [20] for H boson on-shell signal production at NLO in QCD have been used to calibrate the behavior of associated particles in the simulation of off-shell H boson signal at leading order (LO) in QCD, which is described below. The VH and $t\bar{t}H$ production mechanisms of the H boson, which have the smallest expected cross sections, and the subsequent H boson prompt decays are simulated on-shell using PYTHIA 6.4.24 [40].

Four different values of the H boson lifetime have been generated with $c\tau_H = 0, 100, 500, 1000 \mu\text{m}$ for the gluon fusion production mechanism, and these samples are reweighted to model the values of lifetime in between the generated values. The only difference between gluon fusion and the other production mechanisms relevant for the constraint on the lifetime is the H boson p_T spectrum, so reweighting as a function of p_T allows the modeling of the different production mechanisms with nonzero H boson lifetime. Following the formalism in Eq. (4) for spin-zero and including nonzero spin hypotheses, JHUGEN simulations for a variety of H boson production (gluon fusion, VBF, VH, $t\bar{t}H$, $q\bar{q}$) and decay ($H \rightarrow ZZ/Z\gamma^*/\gamma^*\gamma^* \rightarrow 4\ell$) modes have been generated with SM and BSM couplings to validate model independence of the lifetime analysis. This simulation is detailed in Ref. [17].

The off-shell H boson signal and the interference effects with the background are included at LO in QCD for gluon fusion, VBF, and VH mechanisms, while the $t\bar{t}H$ production is highly suppressed at higher masses and is therefore not simulated off-shell [30, 31]. On-shell and off-shell events from gluon fusion production are generated with the MCFM 6.7 [24, 41, 42] and GG2VV 3.1.5 [43] MC generators while those for the VBF and associated production with an electroweak boson V are generated with PHANTOM 1.2.3 [44]. The leptonic decay of the associated V boson is modeled with a reweighting procedure based on the branching ratios of the V boson [45], and the relatively small contribution of HH production is removed from the PHANTOM simulation. Pure signal, pure background, and several mixed samples with signal-background interference have been produced for the analysis of the interference effects. The modeling of the anomalous couplings from Eq. (4) in the off-shell H boson production is performed by reweighting the SM-like samples. An extended MCFM library provided as part of the Matrix Element Likelihood Approach (MELA) package, [35–37], allows for both reweighting and event simulation with anomalous couplings in off-shell H production, and the analytical reweighting for the $f_{\Lambda Q}$ parametrization used in this analysis is identical to reweighting via the MELA package.

Figure 1 illustrates the simulation of the $gg \rightarrow 4\ell$ process with the above technique, which includes H boson off-shell production, its background, and their interference for the five signal models with the a_1 (SM), a_2 , a_3 , Λ_1 , and Λ_Q terms in Eq. (4). In all cases, the on-shell yield

and the width Γ_H are constrained to the SM expectations, and large enhancements are seen in the off-shell region. The four BSM models correspond to the effective fractions $f_{ai} = 1$ defined in Ref. [17] or Eq. (5). When the on-shell contributions of the anomalous couplings are small, cancellation effects in the off-shell region due to their interference with the a_1 term or with the background, as in the case of the Λ_Q term, may suppress the off-shell yield for a given Γ_H . Among these four BSM models, the Λ_Q term results in the largest off-shell enhancement, and only the Λ_Q and a_1 terms, and their interference between each other and the background are considered in the width analysis. Constraints on the a_2 , a_3 , and Λ_1 terms have already been measured from on-shell analyses [17, 18].

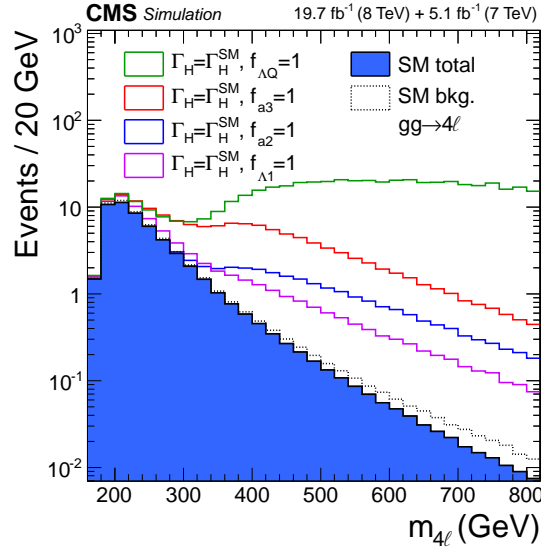


Figure 1: The $m_{4\ell}$ distributions in the off-shell region in the simulation of the $gg \rightarrow 4\ell$ process with the Λ_Q ($f_{\Lambda Q} = 1$), a_3 ($f_{a3} = 1$), a_2 ($f_{a2} = 1$), and Λ_1 ($f_{\Lambda 1} = 1$) terms, as open histograms, as well as the a_1 term (SM), as the filled histogram, from Eq. (4) in decreasing order of enhancement at high $m_{4\ell}$. The on-shell signal yield and the width Γ_H are constrained to the SM expectations. In all cases, the background and its interference with different signal hypotheses are included except in the case of the pure background (dotted), which has greater off-shell yield than the SM signal-background contribution due to destructive interference.

In the case of the off-shell MC simulation, the QCD renormalization and factorization scales are set to the dynamic scales $m_{4\ell}/2$ for gluon fusion and $m_{4\ell}$ for the VBF+VH signal productions and their backgrounds. Higher-order QCD corrections for the gluon fusion signal process are known to an accuracy of next-to-next-to-leading order (NNLO) and next-to-next-to-leading logarithms for the total cross section [30, 31], and to NNLO as a function of $m_{4\ell}$ [46]. The $m_{4\ell}$ -dependent correction factors to the LO cross section (K factors) are typically in the range of 2.0 to 2.7. Although no exact calculation exists beyond the LO for the $gg \rightarrow ZZ$ continuum background, it has been recently shown [47] that the soft collinear approximation is able to describe the background cross section and the interference term at NNLO. Further calculations also show that the K factors are very similar at NLO for the signal and background [48] and at NNLO for the signal and interference terms [49]. Therefore, the same K factor is used for the signal and background [46]. Similarly, QCD and electroweak corrections are known to an accuracy of NNLO for the VBF and VH signal contributions [30, 31, 50], but no calculation exists beyond the LO for the corresponding background contributions. The same K factors as in signal are also assumed for the background and interference contributions. Uncertainties due to the limited theoretical knowledge of the background K factor have a small impact on

the final results.

The background $q\bar{q} \rightarrow ZZ$ process is simulated using POWHEG at NLO in QCD with no interference with H boson signal production. The NLO electroweak calculations [51, 52] predict negative, $m_{4\ell}$ -dependent corrections to this process for on-shell Z boson pairs and are taken into account. In addition, a two-jet inclusive MADGRAPH 5.1.3.30 [53] simulation is used to check jet categorization in the $q\bar{q} \rightarrow ZZ$ process. PYTHIA is used to simulate parton showering and hadronization for all MC signal and background events. The generated MC events are subsequently processed with the CMS full detector simulation, based on GEANT4 [54], and reconstructed using the same algorithm used for the events in data.

The background from Z production with associated jets, denoted as $Z + X$, comes from the production of Z and WZ bosons in association with jets as well as from $t\bar{t}$ production with one or two jets misidentified as an electron or a muon. The estimation of the $Z + X$ background in the four-lepton final state is obtained from data control regions without relying on simulation [16].

4 Event selection

The event reconstruction and selection requirements are the same as those in the previous measurements of the H boson properties in the $H \rightarrow 4\ell$ channel [10, 16, 17, 20]. Only small modifications are made to the lepton impact parameter requirements in the lifetime analysis to retain potential signal with a displaced four-lepton vertex.

As in previous measurements [10, 16, 17, 20], events are triggered by requiring the presence of two leptons (electrons or muons) with asymmetric requirements on their p_T . A triple-electron trigger is also used. Electron candidates are defined by a reconstructed charged-particle track in the tracker pointing to an energy deposition in the ECAL. A muon candidate is identified as a charged-particle track in the muon system that matches a track reconstructed in the tracker. The electron energy is measured primarily from the ECAL cluster energy, while the muon momentum and the charged-lepton impact parameters near the interaction region are measured primarily by the tracker. Electrons and muons are required to be isolated from other charged and neutral particles [16]. Electrons (muons) are reconstructed for $p_T > 7$ (5) GeV within the geometrical acceptance $|\eta| < 2.5$ (2.4) [55, 56]. Trigger and reconstruction efficiencies for muons and electrons are found to be independent on the lifetime of the H boson, similar to other studies of long-lived particles [57, 58].

Events are selected with at least four identified and isolated electrons or muons to form the four-lepton candidate. Two $Z \rightarrow \ell^+\ell^-$ candidates originating from a pair of leptons of the same flavor and opposite charge are required. The $\ell^+\ell^-$ pair with an invariant mass, m_1 , nearest to the nominal Z boson mass is denoted Z_1 and is retained if it is in the range $40 < m_1 < 120$ GeV. A second $\ell^+\ell^-$ pair, denoted Z_2 , is required to have an invariant mass $12 < m_2 < 120$ GeV. If more than one Z_2 candidate satisfies all criteria, the pair of leptons with the highest scalar p_T sum is chosen. The lepton p_T selection is tightened with respect to the trigger by requiring at least one lepton to have $p_T > 20$ GeV, another one to have $p_T > 10$ GeV, and any oppositely charged pair of leptons among the four selected to satisfy $m_{\ell\ell} > 4$ GeV regardless of flavor. A Z boson decay into a lepton pair can be accompanied by final state radiation where the radiated photon is associated to the corresponding lepton to form the Z boson candidate as $Z \rightarrow \ell^+\ell^-\gamma$ [16].

The electrons and muons that comprise the four-lepton candidate are checked for consistency with a reference vertex. In the width analysis, this comparison is done with respect to the

primary vertex of each event, defined as the one passing the standard vertex requirements [59] and having the largest $\sum p_T^2$ of all associated charged tracks. The significance of the three-dimensional impact parameter (SIP) of each lepton, calculated from the track parameters and their uncertainties at the point of closest approach to this primary vertex, is required to be less than 4 [16]. This requirement does not allow for a displaced vertex, so in order to constrain the lifetime of the H boson, the reference of the comparison is switched to the vertex formed by the two leptons from the Z_1 candidate. The SIP of the two leptons from Z_1 is required to be less than 4, and that of the remaining two leptons is required to be less than 5. An additional requirement $\chi_{4\ell}^2/\text{dof} < 6$ for the four-lepton vertex is applied to further suppress the $Z + X$ background. Both analyses also require the presence of the reconstructed proton-proton collision vertex in each event. The combination of these requirements allows for the detection of a displaced H boson decay while keeping the selection efficiencies similar between the two criteria.

After selection, the prompt-decay backgrounds originate from the $q\bar{q} \rightarrow ZZ/Z\gamma^* \rightarrow 4\ell$ and $gg \rightarrow ZZ/Z\gamma^* \rightarrow 4\ell$ processes together with 4ℓ production with associated fermions, such as VBF and associated V production. These backgrounds are evaluated from simulation following Refs. [10, 16]. The $Z + X$ background may include displaced vertices due to b-quark jets and is evaluated using the observed control samples as discussed in Ref. [16], which employs the tight-to-loose lepton misidentification method. While the misidentification rates are consistent between the two different vertex selection requirements, the overall number of selected $Z + X$ background events is about 15% higher when using the vertex requirements of the lifetime measurement. The number of prompt-decay signal and background events is about 2% higher with these lifetime measurement requirements.

In the width analysis, the presence of jets is used as an indication of VBF or associated production with an electroweak boson decaying hadronically, such as WH or ZH. The CMS particle-flow (PF) algorithm [60–63], which combines information from all subdetectors, is used to provide an event description in the form of reconstructed particle candidates. The PF candidates are then used to build jets and lepton isolation quantities. Jets are reconstructed using the anti- k_T clustering algorithm [64] with a distance parameter of 0.5, as implemented in the FASTJET package [65, 66]. Jet energy corrections are applied as a function of the jet p_T and η [67]. An offset correction based on the jet area method is applied to subtract the energy contribution not associated with the high- p_T scattering such as electronic noise and pileup, the latter of which results primarily from other pp collisions in the same bunch crossing [67–69]. Jets are only considered if they have $p_T > 30 \text{ GeV}$ and $|\eta| < 4.7$, and if they are separated from the lepton candidates and identified final-state radiation photons.

Within the tracker acceptance, the jets are reconstructed with the constraint that the charged particles are compatible with the primary vertex. In addition, jets arising from the primary interaction are separated using a multivariate discriminator from those reconstructed due to energy deposits associated with pileup interactions, particularly those from neutral particles not associated with the primary vertex of the event. The discrimination is based on the differences in the jet shapes, the relative multiplicity of charged and neutral components, and the fraction of p_T carried by the hardest components [70]. In the width analysis, the events are split into two categories: those with two or more selected jets (dijet category) and the remaining events (nondijet category). When more than two jets are selected, the two jets with the highest p_T are chosen for further analysis.

The systematic uncertainties in the event selection are generally the same as those investigated in Refs. [10, 16, 17, 20]. Among the yield uncertainties, experimental systematic uncertainties are evaluated from data for the lepton trigger efficiency and the combination of object recon-

struction, identification, and isolation efficiencies. Signal and background uncertainties after the lifetime analysis selection are found to be consistent with the width analysis selection. Most of the signal normalization uncertainties are statistical in nature because the signal strength is left unconstrained and because the systematic uncertainties affect only the relative efficiency of $4e$, 4μ , and $2e2\mu$ reconstruction. The overall predicted signal cross section is, therefore, not directly used in the analysis while the theoretical uncertainties in the 4ℓ background remain unchanged compared to Refs. [10, 16]. The $Z + X$ yield uncertainties are estimated to be 20%, 40%, and 25% for the $4e$, 4μ , and $2e2\mu$ decay channels, respectively, and also remain unchanged compared to Ref. [16].

5 Observables

Several observables, such as the four-lepton invariant mass, $m_{4\ell}$, or the measured lifetime of each H boson candidate, Δt , are used either as input to likelihood fits or to categorize events in this paper. The full list of observables in each category is shown in Table 1, and they are discussed in detail below. The full kinematic information from each event is extracted using the MELA kinematic discriminants, which make use of the correlation between either the two jets and the H boson to identify the production mechanism, or the $H \rightarrow 4\ell$ decay products to identify the decay kinematics. These discriminants use either five, in the case of production, or seven, in the case of decay, mass and angular input observables $\vec{\Omega}$ [35, 37] to describe kinematics at LO in QCD. The p_T of either the combined H boson and 2 jets system for the production discriminant (\mathcal{D}_{jet}) [20] or the H boson itself for the decay discriminants (\mathcal{D}^{kin}) [2] is not included in the input observables in order to reduce associated uncertainties.

Table 1: List of observables, \vec{x} , and categories of events used in the analyses of the H boson lifetime and width. The $\mathcal{D}_{\text{jet}} < 0.5$ requirement is defined for $N_{\text{jet}} \geq 2$, but by convention this category also includes events with less than two selected jets, $N_{\text{jet}} < 2$.

Category	Mass region	Criterion	Observables \vec{x}
Lifetime	$105.6 < m_{4\ell} < 140.6 \text{ GeV}$	Any	Δt \mathcal{D}_{bkg}
Width, on-shell dijet	$105.6 < m_{4\ell} < 140.6 \text{ GeV}$	$N_{\text{jet}} \geq 2$	$m_{4\ell}$ $\mathcal{D}_{\text{bkg}}^{\text{kin}}$ \mathcal{D}_{jet}
Width, on-shell nondijet	$105.6 < m_{4\ell} < 140.6 \text{ GeV}$	$N_{\text{jet}} < 2$	$m_{4\ell}$ $\mathcal{D}_{\text{bkg}}^{\text{kin}}$ p_T
Width, off-shell dijet	$220 < m_{4\ell} < 1600 \text{ GeV}$	$\mathcal{D}_{\text{jet}} \geq 0.5$	$m_{4\ell}$ \mathcal{D}_{gg}
Width, off-shell nondijet	$220 < m_{4\ell} < 1600 \text{ GeV}$	$\mathcal{D}_{\text{jet}} < 0.5$	$m_{4\ell}$ \mathcal{D}_{gg}

The discriminant sensitive to the VBF signal topology is calculated as

$$\mathcal{D}_{\text{jet}} = \left[1 + \frac{\mathcal{P}_{\text{HJJ}}(\vec{\Omega}^{\text{H+JJ}}, m_{4\ell})}{\mathcal{P}_{\text{VBF}}(\vec{\Omega}^{\text{H+JJ}}, m_{4\ell})} \right]^{-1}, \quad (6)$$

where \mathcal{P}_{VMF} and \mathcal{P}_{HJJ} are probabilities obtained from the JHUGEN matrix elements for the VBF process and gluon fusion in association with two jets ($H + 2\text{jets}$) within the MELA framework [20]. This discriminant is equally efficient in separating VBF from either $gg \rightarrow H + 2\text{jets}$ signal or gg or $q\bar{q} \rightarrow 4\ell + 2\text{jets}$ background because jet correlations in these processes are distinct from the VBF process.

In the on-shell region, the \mathcal{D}_{jet} discriminant is one of the width analysis observables used in the dijet category. The \mathcal{D}_{jet} distribution shown in Fig. 2 (left) is used to distinguish gluon fusion, VBF, and VH production mechanisms in this category. The p_T of the 4ℓ system is used to distinguish the production mechanism of the remaining on-shell events in the nondijet category.

In the off-shell region, the requirement $\mathcal{D}_{\text{jet}} \geq 0.5$ is applied instead, keeping nearly half of the VBF events and less than 4% of all other processes, with only a small dependence on $m_{4\ell}$. Events that fail this requirement enter the nondijet category in the off-shell region. The different treatment of \mathcal{D}_{jet} between the on-shell and off-shell regions keeps the observables the same as in the previous width analysis [10].

Uncertainties in modeling the jet distributions affect the separation of events between the two dijet categories but do not affect the combined yield of either signal or background events. For the on-shell dijet category, a 30% normalization uncertainty is taken into account for the $gg \rightarrow H + 2\text{jets}$ signal cross section while the uncertainty in the selection of two or more jets from VBF production is 10%. The \mathcal{D}_{jet} distribution uncertainties other than those for $Z + X$ are estimated by comparing alternative MC generators and tunings, where smaller effects from uncertainties due to jet energy scale and resolution are also included.

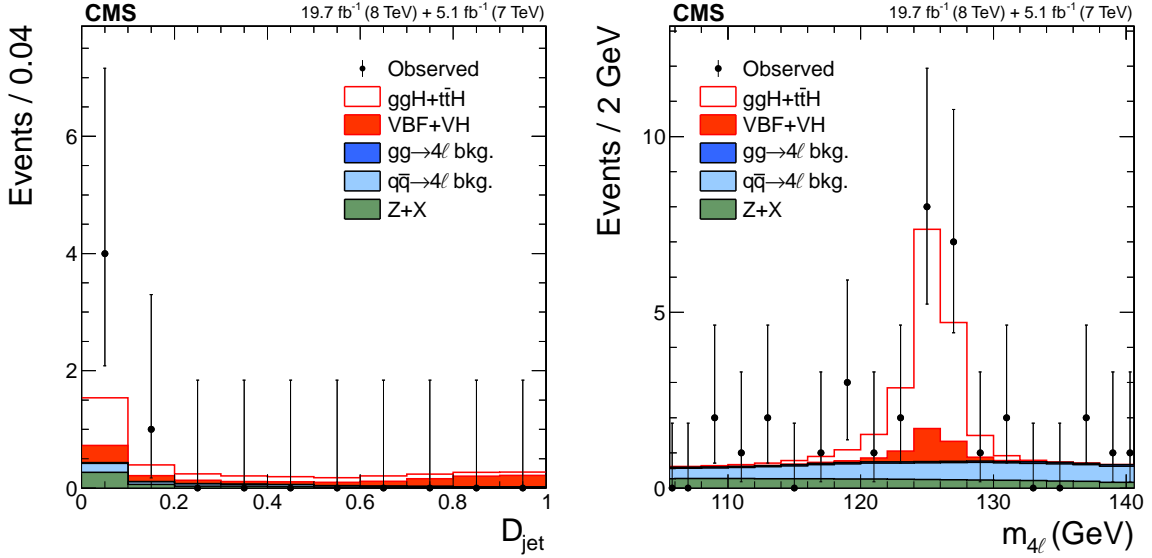


Figure 2: Distributions of the four-lepton invariant mass \mathcal{D}_{jet} (left) and $m_{4\ell}$ (right) in the on-shell region of the H boson width analysis. The \mathcal{D}_{jet} distributions show events in the dijet category with a requirement $120 < m_{4\ell} < 130$ GeV. The $m_{4\ell}$ distributions combine the nondijet and dijet categories, the former with an additional requirement $\mathcal{D}_{\text{bkg}}^{\text{kin}} > 0.5$ to suppress the dominant $q\bar{q} \rightarrow 4\ell$ background. The points with error bars represent the observed data, and the histograms represent the expected contributions from the SM backgrounds and the H boson signal. The contribution from the VBF and VH production is shown separately.

In the off-shell region, the uncertainties in the \mathcal{D}_{jet} distribution imply uncertainties in the categorization requirement $\mathcal{D}_{\text{jet}} > 0.5$. To determine the uncertainty in the dijet selection, NLO QCD simulation with POWHEG is compared to the two LO generators PHANTOM and JHUGEN for the VBF production, all with parton showering simulated with PYTHIA. For this comparison, VH production is omitted from the PHANTOM simulation since no events in association with electroweak boson production pass the $\mathcal{D}_{\text{jet}} \geq 0.5$ requirement. The efficiency of categorization for VBF-like events is stable within 5%, and the main difference comes from the uncertainty in the additional jet radiation after the hadronization of simulated events at LO or NLO in QCD using PYTHIA. A similar comparison of the signal production in gluon fusion is performed between the POWHEG simulations at NLO in QCD with and without the MINLO procedure for multijet simulation, and two LO generators MCFM and GG2VV. With proper matching of the hadronization scale for the LO generators in PYTHIA [71], a good agreement within 15% is found between all generators, with absolute dijet categorization efficiency of ap-

proximately 3%. The $m_{4\ell}$ dependence of the categorization efficiency is found to be similar between the different generators.

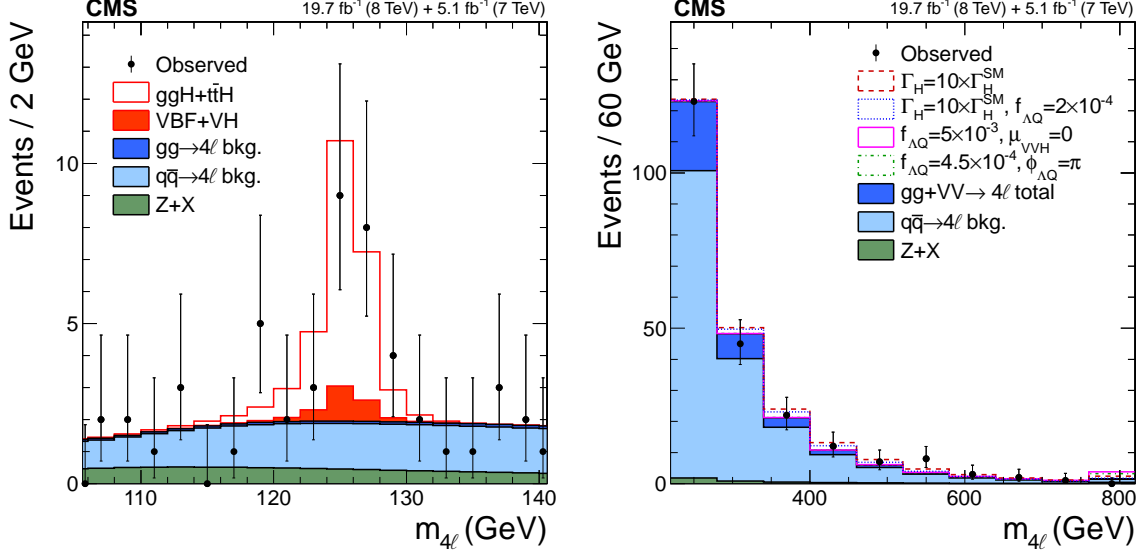


Figure 3: Distributions of the four-lepton invariant mass $m_{4\ell}$ in the on-shell (left) and off-shell (right) regions of the H boson width analysis for all observed and expected events. The points with error bars represent the observed data in both on-shell and off-shell region distributions. The histograms for the on-shell region represent the expected contributions from the SM backgrounds and the H boson signal with the contribution from the VBF and VH production shown separately. The filled histograms for the off-shell region represent the expected contributions from the SM backgrounds and H boson signal, combining gluon fusion, VBF, and VH processes. Alternative H boson width and coupling scenarios are shown as open histograms with the assumption $\phi_{\Lambda Q} = 0$ unless specified otherwise, and the overflow bin includes events up to $m_{4\ell} = 1600$ GeV.

With the above uncertainties, the contributions of the signal, background, and their interference in the off-shell region for each category are obtained with the PHANTOM generator for the VBF and associated electroweak boson production, and with the MCFM generator for the gluon fusion production. The dijet categorization efficiency as a function of $m_{4\ell}$ is reweighted to the POWHEG + MINLO prediction for gluon fusion signal contribution, and the same reweighting is used in the background and interference contributions. For the $q\bar{q} \rightarrow ZZ$ background, the comparison of the NLO QCD simulation with POWHEG with the two-jet inclusive MADGRAPH simulation leads to a 25% uncertainty in the dijet categorization. Both dijet categorization and its uncertainty have negligible $m_{4\ell}$ dependence, and the dijet categorization efficiency is around 0.6%. An uncertainty of 100% is assigned to the categorization of $Z + X$ events, primarily due to statistical limitations in the data-driven estimate. This uncertainty has a negligible contribution to the results since the contribution of $Z + X$ is small in the total off-shell expected yield and negligible in the dijet category.

The discriminant sensitive to the $gg \rightarrow 4\ell$ kinematics is calculated as

$$\mathcal{D}^{\text{kin}} = \left[1 + \frac{\alpha \mathcal{P}_{\text{bkg}}^{q\bar{q}}(\vec{\Omega}^{\text{H} \rightarrow 4\ell}, m_{4\ell})}{\mathcal{P}_{\text{sig}}^{\text{gg}}(\vec{\Omega}^{\text{H} \rightarrow 4\ell}, m_{4\ell}) + \sqrt{\beta} \mathcal{P}_{\text{int}}^{\text{gg}}(\vec{\Omega}^{\text{H} \rightarrow 4\ell}, m_{4\ell}) + \beta \mathcal{P}_{\text{bkg}}^{\text{gg}}(\vec{\Omega}^{\text{H} \rightarrow 4\ell}, m_{4\ell})} \right]^{-1}, \quad (7)$$

where the denominator contains the sum of the probability contributions from the signal ($\mathcal{P}_{\text{sig}}^{\text{gg}}$), the background ($\mathcal{P}_{\text{bkg}}^{\text{gg}}$), and their interference ($\mathcal{P}_{\text{int}}^{\text{gg}}$) to the total $gg \rightarrow 4\ell$ process, and

the numerator includes the probability for the $q\bar{q} \rightarrow 4\ell$ background process, all calculated either with the JHUGEN or MCFM matrix elements within the MELA framework [10, 16, 17]. The two coefficients α and β are tuned differently in the on-shell and off-shell width analysis samples. Signal-background interference effects are negligible in the on-shell region, so the kinematic discriminant is tuned to isolate signal from the dominant background process with $\mathcal{D}_{\text{bkg}}^{\text{kin}} = \mathcal{D}^{\text{kin}}(\alpha = 1, \beta = 0)$ [2, 36]. In the off-shell region, the discriminant is tuned to isolate the full gluon fusion process, including the interference term, for the ratio $\Gamma_{\text{H}}^{\text{SM}}/\Gamma_{\text{H}} \sim \alpha = \beta = 0.1$ close to the expected sensitivity of the analysis. The discriminant is therefore labeled as $\mathcal{D}_{\text{gg}} = \mathcal{D}^{\text{kin}}(\alpha = \beta = 0.1)$ [10].

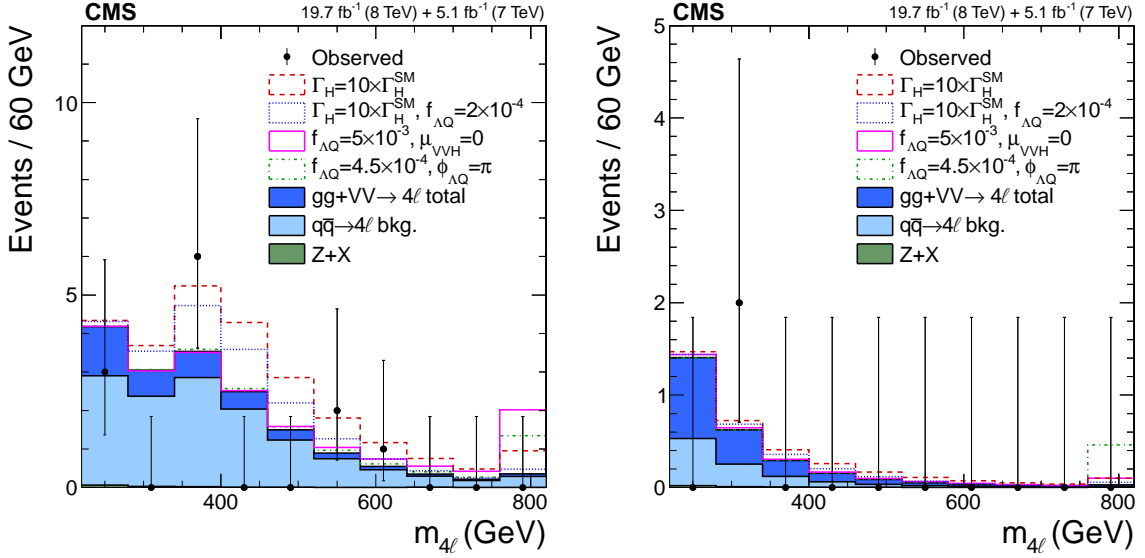


Figure 4: Distribution of the four-lepton invariant mass $m_{4\ell}$ in the off-shell region in the nondijet (left) and dijet (right) categories. A requirement $\mathcal{D}_{\text{gg}} > 2/3$ is applied in the nondijet category to suppress the dominant $q\bar{q} \rightarrow 4\ell$ background. The points with error bars represent the observed data, and the filled histograms represent the expected contributions from the SM backgrounds and H boson signal, combining gluon fusion, VBF, and VH processes. Alternative H boson width and coupling scenarios are shown as open histograms. The overflow bins include events up to $m_{4\ell} = 1600$ GeV, and $\phi_{\Lambda Q} = 0$ is assumed where it is unspecified.

Apart from the above kinematic discriminants and p_T , the width analysis employs the four-lepton invariant mass $m_{4\ell}$ as the main observable, which provides signal and background separation in the on-shell region and which is sensitive to the Γ_{H} values and anomalous couplings in the off-shell region. The $m_{4\ell}$ distributions are illustrated in Fig. 3 for the on-shell and off-shell regions without any kinematic requirements, Fig. 2 (right) for the on-shell region with the requirement $\mathcal{D}_{\text{bkg}}^{\text{kin}} > 0.5$, and Fig. 4 for the two event categories in the off-shell region, with the requirement $\mathcal{D}_{\text{gg}} > 2/3$ on the nondijet category. The requirements on the kinematic discriminants $\mathcal{D}_{\text{bkg}}^{\text{kin}}$ or \mathcal{D}_{gg} suppress the relative contribution of background in the illustration of event distributions. In the lifetime analysis, the $m_{4\ell}$ and $\mathcal{D}_{\text{bkg}}^{\text{kin}}$ observables are combined into one, called \mathcal{D}_{bkg} [14, 17, 37], in order to reduce the number of observables. It is constructed by multiplying the matrix element probability ratio in Eq. (7) by the ratio of probabilities for $m_{4\ell}$ from the nonresonant $q\bar{q} \rightarrow 4\ell$ process and the resonant production $gg \rightarrow \text{H} \rightarrow 4\ell$ for the measured $m_{\text{H}} = 125.6$ GeV. The \mathcal{D}_{bkg} distribution in the lifetime analysis is shown in Fig. 5. To account for the lepton momentum scale and resolution uncertainty in the $m_{4\ell}$ or \mathcal{D}_{bkg} distributions, alternative signal distributions are taken from the variations of both of these contributions.

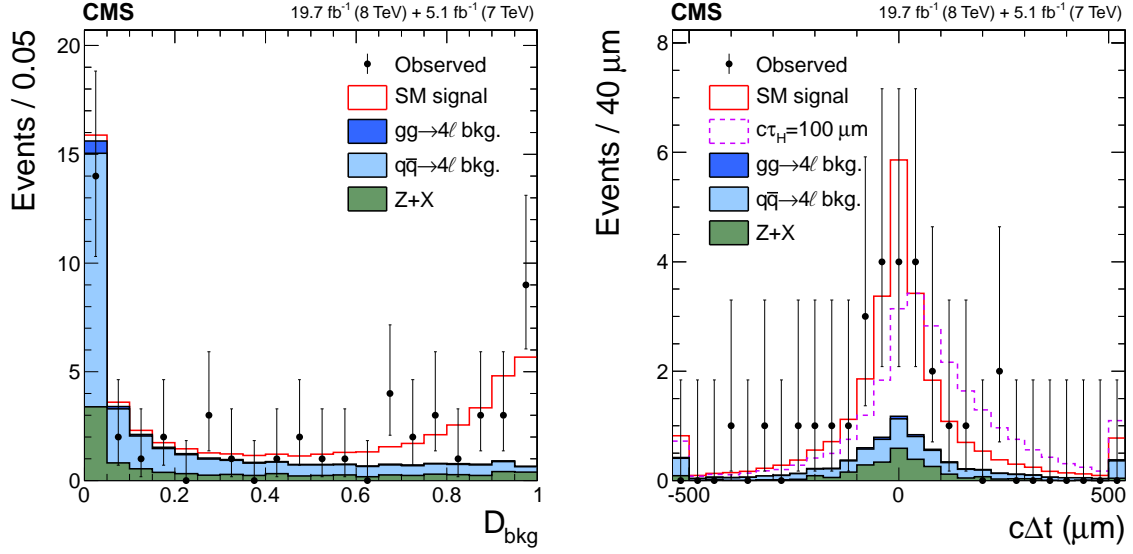


Figure 5: Distributions of \mathcal{D}_{bkg} (left) and $c\Delta t$ (right) in the lifetime analysis with $\mathcal{D}_{\text{bkg}} > 0.5$ required for the latter to suppress the background. The points with error bars represent the observed data, and the filled histograms stacked on top of each other represent the expected contributions from the SM backgrounds. Stacked on the total background contribution, the open histograms show the combination of all production mechanisms expected in the SM for the H boson signal with either the SM lifetime or $c\tau_{\text{H}} = 100 \mu\text{m}$. Each signal contribution in the different open histograms are the same as the total number of events expected from the combination of all production mechanisms in the SM. All signal distributions are shown with the total number of events expected in the SM. The first and last bins of the $c\Delta t$ distributions include all events beyond $|c\Delta t| > 500 \mu\text{m}$.

The lifetime analysis makes use of the observable Δt calculated following Eq. (1). The reference point for H boson production vertex is taken to be the beam spot, which is the pp collision point determined by fitting charged-particle tracks from events in multiple collisions, and the value of $\Delta\vec{r}_{\text{T}}$ is calculated as the displacement from the beam spot to the 4ℓ vertex in the plane transverse to the beam axis. An alternative calculation of Δt has also been considered using the primary vertex of each event instead of the beam spot, but the different associated particles in the H boson production and their multiplicity would introduce additional model dependence in the primary vertex resolution.

The Δt value is non-negative and follows the exponential decay distribution if it is known perfectly for each event. However, resolution effects arising mostly from limited precision of the $\Delta\vec{r}_{\text{T}}$ measurement allow negative Δt values. This feature allows for an effective self-calibration of the resolution from the data. Symmetric broadening of the Δt distribution indicates resolution effects while positive skew indicates sizable signal lifetime. Figure 5 displays the Δt distributions. The resolution in Δt also depends on the p_{T} spectrum of the produced H boson, which differs among the production mechanisms, and this dependence is accounted for in the fit procedure as described in detail in Sec. 6. The distributions of Δt and p_{T} are shown in Figs. 5 and 6, respectively. Since the discriminant \mathcal{D}_{bkg} is optimal for signal separation in the on-shell region, a requirement $\mathcal{D}_{\text{bkg}} > 0.5$ is applied to reduce the background when showing these distributions.

Uncertainties in the Δt distribution for the signal and the prompt background are obtained from a comparison of the expected and observed distributions in the $m_{4\ell}$ sidebands, $70 < m_{4\ell} < 105.6 \text{ GeV}$ and $170 < m_{4\ell} < 800 \text{ GeV}$. These uncertainties obtained from this comparison

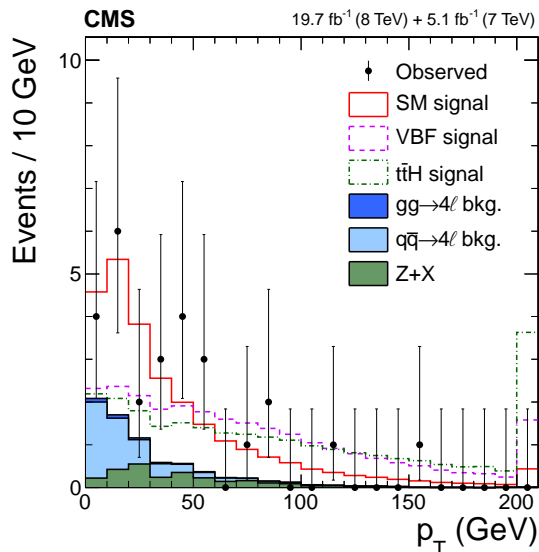


Figure 6: Distributions of the four-lepton p_T with the selection used in the lifetime analysis and the requirement $\mathcal{D}_{\text{bkg}} > 0.5$ to suppress the backgrounds. The points with error bars represent the observed data, and the filled histograms stacked on top of each other represent the expected contributions from the SM backgrounds. Stacked on the total background contribution, the open histograms show the H boson signal either with the combination of all production mechanisms expected in the SM, or for the VBF or $t\bar{t}H$ production mechanisms. Each signal contribution in the different open histograms is normalized to the total number of events expected from the combination of all production mechanisms in the SM. The overflow bin includes all events beyond $p_T > 200$ GeV.

correspond to varying the Δt resolution by $+17/-15\%$, $+14/-12\%$, and $+20/-17\%$ for the $4e$, 4μ , and $2e2\mu$ final states, respectively. The $Z + X$ parametrization is obtained from the control region in the analysis mass range $105.6 < m_{4\ell} < 140.6$ GeV, and its alternative parametrization obtained from the control region events in the mass range $140.6 < m_{4\ell} < 170$ GeV reflects the uncertainties in the data-driven estimate. A cross-check of the Δt distributions is also performed with the 3ℓ control samples enriched in WZ prompt decay, and the distributions are found to be consistent with simulation.

6 Constraints on the lifetime

The H boson lifetime analysis is based on two observables $\vec{x} = (\Delta t, \mathcal{D}_{\text{bkg}})$, which allow the measurement of the average signal lifetime τ_H and the discrimination of the H boson signal from background using a simultaneous likelihood fit. The extended likelihood function is defined for N_{ev} candidate events as

$$\mathcal{L} = \exp\left(-n_{\text{sig}} - \sum_k n_{\text{bkg}}^{(k)}\right) \prod_i^{N_{\text{ev}}} \left(n_{\text{sig}} \mathcal{P}_{\text{sig}}(\vec{x}_i; \vec{\zeta}) + \sum_k n_{\text{bkg}}^{(k)} \mathcal{P}_{\text{bkg}}^{(k)}(\vec{x}_i; \vec{\zeta}) \right), \quad (8)$$

where n_{sig} is the number of signal events and n_{bkg}^k is the number of background events of type k ($gg \rightarrow 4\ell$, $q\bar{q} \rightarrow 4\ell$, $Z + X$). The probability density functions \mathcal{P}_{sig} for signal, and $\mathcal{P}_{\text{bkg}}^k$ for each background process k are described as histograms (templates). The likelihood parametrization is constructed independently in each of the $4e$, 4μ , or $2e2\mu$ final states, and for 7 and 8 TeV pp collision energy. The parameters $\vec{\zeta}$ for the signal and $\vec{\zeta}$ for the background

processes include parametrization uncertainties, and $\vec{\zeta}$ also includes τ_H as the parameter of interest. The likelihood in Eq. (8) is maximized with respect to the parameters $n_{\text{sig}}, n_{\text{bkg}}^k, \vec{\zeta}$ and $\vec{\zeta}$, which constitute the nuisance parameters and the parameter of interest. The nuisance parameters are either constrained within the associated uncertainties or left unconstrained in the fit.

The kinematics of the four-lepton decay, affecting \mathcal{D}_{bkg} , and the four-lepton vertex position and resolution, affecting Δt , are found to be independent. Therefore, the two-dimensional probability distributions of $\mathcal{P}(\Delta t, \mathcal{D}_{\text{bkg}})$ are constructed as the product of two one-dimensional distributions. In the case of the signal probability, the Δt templates are conditional on the parameter of interest τ_H . The signal Δt parametrization is obtained for the range $0 \leq c\tau_H \leq 1000 \mu\text{m}$ by reweighting the simulation available for the gluon fusion process at $c\tau_H = 0, 100, 500, \text{ and } 1000 \mu\text{m}$ to $c\tau_H$ values in steps of $10 \mu\text{m}$ and interpolating linearly for any intermediate value.

The Δt parametrization for all SM H boson production mechanisms (gluon fusion, VBF, WH, ZH, and $t\bar{t}H$) is obtained by reweighting gluon fusion production events as a function of p_T at each of the τ_H values. This procedure reproduces Δt resolution effects predicted from the simulation for prompt signal (i.e. $\tau_H = 0$) and is, therefore, valid for nonzero lifetime. As shown in Fig. 6, the gluon fusion production mechanism has the softest p_T spectrum while $t\bar{t}H$ production yields the hardest p_T , and the distribution of Δt is thus wider in gluon fusion and narrower in $t\bar{t}H$ production, with other production mechanisms in between. Gluon fusion production and $t\bar{t}H$ distributions, with their respective yields scaled to the total SM production cross section, are therefore taken as the two extreme variations while the nominal Δt distribution is parametrized with the SM combination of the different production mechanisms. The Δt distribution used in the likelihood is varied from the nominal prediction between these two extremes with a continuous production parameter included in $\vec{\zeta}$ in Eq. (8). Any other production mechanism or a mixture can be described with this parametrization, and the values of the production parameter corresponding to the p_T spectrum of either pure VBF, WH, ZH, or $t\bar{t}H$ mechanisms are excluded at more than 95% CL from a fit to data. This information is consistent with the observed p_T spectrum in Fig. 6.

While the Δt and \mathcal{D}_{bkg} parametrizations are obtained for the SM couplings in the $H \rightarrow ZZ \rightarrow 4\ell$ decay, and for p_T spectra as in SM-like production mechanisms (gluon fusion, VBF, WH, ZH, and $t\bar{t}H$), the analysis has little dependence on anomalous couplings in either the production or the decay of the H boson. It has already been established [17] that the kinematics of the $H \rightarrow 4\ell$ decay are consistent with the kinematics of the SM H boson decay and inconsistent with a wide range of exotic models. The Δt and \mathcal{D}_{bkg} distributions have little variation within the allowed range of exotic couplings in the $H \rightarrow 4\ell$ decay. The expected τ_H constraint remains stable within 10% when the simulation for those exotic models is tested instead of the simulation with SM couplings. Anomalous couplings in production are found to have a substantial effect on the p_T spectrum, typically making the spectrum harder in the VBF, WH, ZH, and $t\bar{t}H$ production mechanisms. Extreme variations in the p_T spectrum, however, are already excluded by the data, and p_T variations allowed by the data are reflected in the Δt parametrization with the parameter describing the production mechanisms.

Figure 7 shows the likelihood distribution as a function of $c\tau_H$. The allowed 68% and 95% CL intervals are defined using the respective profile likelihood function values $-2 \ln(\mathcal{L}/\mathcal{L}_{\text{max}}) = 1.00$ and 3.84 for which exact coverage is expected in the asymptotic limit [72]. The approximate coverage has been tested with the generated samples at different $c\tau_H$ values, and the quoted results have been found to be conservative. The observed (expected) average lifetime is $c\tau_H =$

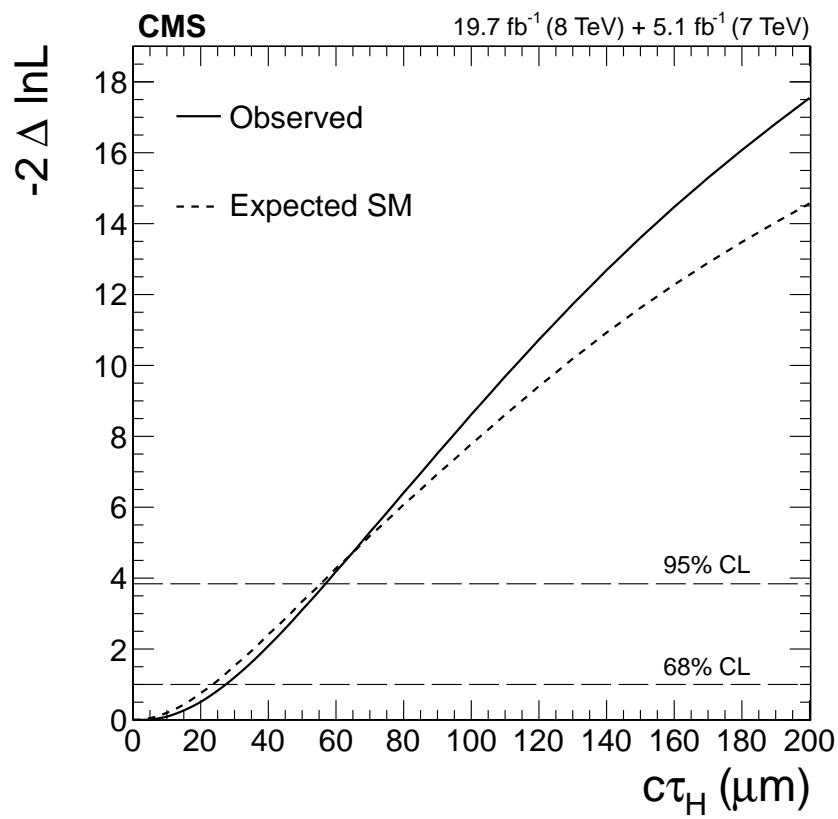


Figure 7: Observed (solid) and expected (dashed) distributions of $-2 \ln(\mathcal{L}/\mathcal{L}_{\max})$ as a function of the H boson average lifetime $c\tau_H$.

2_{-2}^{+25} (0_{-0}^{+24}) μm ($\tau_{\text{H}} = 10_{-10}^{+80}$ fs for the observation and $\tau_{\text{H}} = 0_{-0}^{+80}$ fs for the expectation), and the allowed region at the 95% CL is $c\tau_{\text{H}} < 57$ (56) μm ($\tau_{\text{H}} < 190$ fs for both the observation and the expectation). The observed number of signal events remains consistent with Ref. [16]. The observed (expected) upper limit on the average lifetime at 95% CL corresponds through Eq. (2) to the lower limit on the H boson width $\Gamma_{\text{H}} > 3.5 \times 10^{-9}$ MeV ($\Gamma_{\text{H}} > 3.6 \times 10^{-9}$ MeV) regardless of the value of $f_{\Lambda Q}$.

7 Constraints on the width

The H boson width Γ_{H} and the effective fraction $f_{\Lambda Q}$ for the Λ_Q anomalous coupling are measured in an unbinned maximum likelihood fit of a signal-plus-background model following Eq. (8). In addition to the event categories already defined in the lifetime analysis for the final states and pp collision energy, events are also split into dijet and nondijet categories, and into on-shell and off-shell regions. In the on-shell region, a three-dimensional distribution of $\vec{x} = (m_{4\ell}, \mathcal{D}_{\text{bkg}}^{\text{kin}}, p_{\text{T}}$ or \mathcal{D}_{jet}) is analyzed, following the methodology described in Ref. [16]. In the off-shell region, a two-dimensional distribution $\vec{x} = (m_{4\ell}, \mathcal{D}_{\text{gg}})$ is analyzed following the methodology described in Ref. [10] with the events split into the two dijet categories defined in Table 1.

The probability distribution functions are built using the full detector simulation or data control regions and are defined for both the signal (\mathcal{P}_{sig}) and the background (\mathcal{P}_{bkg}) contributions as well as their interference (\mathcal{P}_{int}), as a function of the observables \vec{x} discussed above. Several production mechanisms such as gluon fusion (gg), VBF, WH and ZH (VH) are considered for the signal. The total probability distribution function for the off-shell region is written as

$$\begin{aligned} \mathcal{P}_{\text{tot}}^{\text{off-shell}}(\vec{x}; \Gamma_{\text{H}}, f_{\Lambda Q}) = & \left[\mu_{\text{ggH}} \frac{\Gamma_{\text{H}}}{\Gamma_0} \mathcal{P}_{\text{sig}}^{\text{gg}}(\vec{x}; f_{\Lambda Q}) + \sqrt{\mu_{\text{ggH}} \frac{\Gamma_{\text{H}}}{\Gamma_0}} \mathcal{P}_{\text{int}}^{\text{gg}}(\vec{x}; f_{\Lambda Q}) + \mathcal{P}_{\text{bkg}}^{\text{gg}}(\vec{x}) \right] \\ & + \left[\mu_{\text{VVH}} \frac{\Gamma_{\text{H}}}{\Gamma_0} \mathcal{P}_{\text{sig}}^{\text{VV}}(\vec{x}; f_{\Lambda Q}) + \sqrt{\mu_{\text{VVH}} \frac{\Gamma_{\text{H}}}{\Gamma_0}} \mathcal{P}_{\text{int}}^{\text{VV}}(\vec{x}; f_{\Lambda Q}) + \mathcal{P}_{\text{bkg}}^{\text{VV}}(\vec{x}) \right] \\ & + \mathcal{P}_{\text{bkg}}^{\text{q}\bar{\text{q}}}(\vec{x}) + \mathcal{P}_{\text{bkg}}^{\text{ZZ}}(\vec{x}), \quad (9) \end{aligned}$$

where Γ_0 is a reference value used in simulation and VV stands for a combination of VBF and associated electroweak boson production taken together. Under the assumption $\phi_{\Lambda Q} = 0$ or π , any contribution to the HVV scattering amplitude in Eq. (4) from the a_1 term is proportional to $\sqrt{1 - f_{\Lambda Q}}$ while that from the Λ_Q term is proportional to $\sqrt{f_{\Lambda Q}} \cos(\phi_{\Lambda Q})$. The dependence on $f_{\Lambda Q}$ in Eq. (9) can thus be parametrized with the factor

$$\left(\sqrt{1 - f_{\Lambda Q}} - \sqrt{f_{\Lambda Q}} \cos(\phi_{\Lambda Q}) \frac{m_{4\ell}^2}{m_{\text{H}}^2} \right)^N, \quad (10)$$

where the power N depends on the power of the HVV couplings. The couplings appear twice in the VBF and VH cases, in both production and decay, so the power of the factor is twice as large. Thus, for gluon fusion, $N = 1$ for the interference component ($\mathcal{P}_{\text{int}}^{\text{gg}}$) and $N = 2$ for the signal ($\mathcal{P}_{\text{sig}}^{\text{gg}}$); for VBF and VH, $N = 2$ ($\mathcal{P}_{\text{int}}^{\text{VV}}$) and 4 ($\mathcal{P}_{\text{sig}}^{\text{VV}}$), respectively. Both HZZ and HWW couplings contribute to the VBF and VH production couplings, and this analysis assumes the same Λ_Q would contribute to the HZZ and HWW couplings in Eq. (4). The effective fraction $f_{\Lambda Q}$ is therefore the same for the HZZ and HWW amplitudes.

In the on-shell region, the parametrization includes the small contribution of the $t\bar{t}H$ production mechanism, which is related to the gluon fusion production. The total probability distribution function for the on-shell region is

$$\mathcal{P}_{\text{tot}}^{\text{on-shell}}(\vec{x}) = \mu_{\text{ggH}} \mathcal{P}_{\text{sig}}^{\text{gg}+\text{t}\bar{t}\text{H}}(\vec{x}) + \mu_{\text{VVH}} \mathcal{P}_{\text{sig}}^{\text{VV}}(\vec{x}) + \mathcal{P}_{\text{bkg}}^{\text{q}\bar{\text{q}}}(\vec{x}) + \mathcal{P}_{\text{bkg}}^{\text{gg}}(\vec{x}) + \mathcal{P}_{\text{bkg}}^{\text{ZZ}}(\vec{x}). \quad (11)$$

The normalization of the signal and background distributions is incorporated in the probability functions \mathcal{P} in Eqs. (9) and (11), but the overall signal yield is left unconstrained with the independent signal strength parameters μ_{ggH} and μ_{VVH} , corresponding to the H production mechanisms through coupling to either fermions or weak vector bosons, respectively. The observed μ_{ggH} and μ_{VVH} values are found to be consistent with those obtained in Refs. [10, 16].

The allowed 68% and 95% CL intervals are defined using the profile likelihood function values $-2 \ln(\mathcal{L}/\mathcal{L}_{\text{max}}) = 2.30$ and 5.99 , respectively, for the two-parameter constraints presented, and $-2 \ln(\mathcal{L}/\mathcal{L}_{\text{max}}) = 1.00$ and 3.84 , respectively, for the one-parameter constraints. Exact coverage is expected in the asymptotic limit [72], and the approximate coverage has been tested at several different parameter values with the quoted results having been found to be conservative. The observed distribution of the likelihood as a two-parameter function of Γ_{H} and $f_{\Lambda Q} \cos \phi_{\Lambda Q}$, with $\phi_{\Lambda Q} = 0$ or π , is shown in Fig. 8. Also shown is the one-parameter, conditional likelihood scan of $f_{\Lambda Q} \cos \phi_{\Lambda Q}$ for a given Γ_{H} , where the $-2 \ln(\mathcal{L}/\mathcal{L}_{\text{max}})$ distribution is shown for \mathcal{L}_{max} adjusted according to the most likely value of $f_{\Lambda Q} \cos \phi_{\Lambda Q}$ at the given value of Γ_{H} . The observed and expected likelihood distributions as a function of Γ_{H} are shown in Fig. 9, where $f_{\Lambda Q}$ is either constrained to zero or left unconstrained. The observed (expected) central values with 68% CL uncertainties are $\Gamma_{\text{H}} = 2_{-2}^{+9} (4_{-4}^{+17})$ MeV with $f_{\Lambda Q} = 0$, and $\Gamma_{\text{H}} = 2_{-2}^{+15} (4_{-4}^{+30})$ MeV with $f_{\Lambda Q}$ unconstrained and $\phi_{\Lambda Q} = 0$ or π . The observed (expected) constraints at 95% CL are $\Gamma_{\text{H}} < 26 (41)$ MeV with $f_{\Lambda Q} = 0$, and $\Gamma_{\text{H}} < 46 (73)$ MeV with $f_{\Lambda Q}$ unconstrained and $\phi_{\Lambda Q} = 0$ or π . These observed (expected) upper limits on the H boson width at 95% CL correspond through Eq. (2) to the lower limits on the H boson average lifetime $\tau_{\text{H}} > 2.5 \times 10^{-8} (1.6 \times 10^{-8})$ fs with $f_{\Lambda Q} = 0$ and $\tau_{\text{H}} > 1.4 \times 10^{-8} (9 \times 10^{-9})$ fs with $f_{\Lambda Q}$ unconstrained and $\phi_{\Lambda Q} = 0$ or π .

The result with the constraint $f_{\Lambda Q} = 0$ is consistent with the earlier one from the $H \rightarrow ZZ \rightarrow 4\ell$ channel [10]. It can be reinterpreted as an off-shell signal strength with the change of parameters $\mu_{\text{VVH}}^{\text{off-shell}} = \mu_{\text{VVH}} \Gamma_{\text{H}}/\Gamma_{\text{H}}^{\text{SM}}$, provided the signal strength μ_{VVH} for the on-shell region is uncorrelated with the signal strength $\mu_{\text{VVH}}^{\text{off-shell}}$ for the off-shell region in the likelihood scan. The observed (expected) central values and the 68% CL uncertainties of Γ_{H} with the $f_{\Lambda Q} = 0$ constraint correspond to $\mu_{\text{ggH}}^{\text{off-shell}} = 0.5_{-0.5}^{+2.2} (1.0_{-1.0}^{+5.1})$ and $\mu_{\text{VVH}}^{\text{off-shell}} = 0.4_{-0.4}^{+10.5} (1.0_{-1.0}^{+20.6})$, and the observed (expected) constraints at 95% CL become $\mu_{\text{ggH}}^{\text{off-shell}} < 6.2 (9.3)$ and $\mu_{\text{VVH}}^{\text{off-shell}} < 31.3 (44.4)$. There is no constraint on the ratio $\mu_{\text{VVH}}^{\text{off-shell}}/\mu_{\text{ggH}}^{\text{off-shell}}$ at 68% CL. The Γ_{H} limits with $f_{\Lambda Q}$ unconstrained are weaker because a small nonzero value $f_{\Lambda Q} \sim 2 \times 10^{-4}$ leads to destructive interference between the a_1 and Λ_Q terms in Eq. (4) when $\phi_{\Lambda Q} = 0$. This interference reduces the expected signal yield at these parameter values, thereby reducing the exclusion power for $\Gamma_{\text{H}} > \Gamma_{\text{H}}^{\text{SM}}$. This effect is also illustrated in Fig. 4.

No constraint on $f_{\Lambda Q}$ can be obtained in the limit $\Gamma_{\text{H}} \rightarrow 0$ because, as displayed in Fig. 8, the number of expected off-shell events vanishes. The constraints on $f_{\Lambda Q} \cos \phi_{\Lambda Q}$ given particular Γ_{H} values become tighter for increasing Γ_{H} . The limits on $f_{\Lambda Q} \cos \phi_{\Lambda Q}$ with the assumption $\Gamma_{\text{H}} = \Gamma_{\text{H}}^{\text{SM}}$ are presented in Fig. 9. The observed (expected) value is $f_{\Lambda Q} \cos \phi_{\Lambda Q} = 0_{-0.4}^{+1.0} (0_{-0.4}^{+1.1}) \times 10^{-3}$, and the allowed region at 95% CL is $[-2.4, 3.8] \times 10^{-3}$ ($[-3.6, 4.4] \times 10^{-3}$).

8 Conclusions

Constraints on the lifetime and the width of the H boson are obtained from $H \rightarrow ZZ \rightarrow 4\ell$ events using the data recorded by the CMS experiment during the LHC run 1. The measurement of the H boson lifetime is derived from its flight distance in the CMS detector with the upper bound $\tau_H < 190$ fs at the 95% CL, corresponding to a lower bound on the width $\Gamma_H > 3.5 \times 10^{-9}$ MeV. The measurement of the width is obtained from an off-shell production technique, generalized to include additional anomalous couplings of the H boson to two electroweak bosons. This measurement provides a joint constraint on the H boson width and a parameter that quantifies an anomalous coupling contribution through an on-shell cross-section fraction $f_{\Lambda Q}$. The observed limit on the H boson width is $\Gamma_H < 46$ MeV at the 95% CL with $f_{\Lambda Q}$ left unconstrained while it is $\Gamma_H < 26$ MeV at the 95% CL for $f_{\Lambda Q} = 0$. The constraint $f_{\Lambda Q} < 3.8 \times 10^{-3}$ at the 95% CL is obtained assuming the H boson width expected in the SM, and the $f_{\Lambda Q}$ constraints given any other width value are also presented. Table 2 summarizes the width and corresponding lifetime limits, and Table 3 summarizes the limits on $f_{\Lambda Q}$ under the different $\phi_{\Lambda Q}$ scenarios that can be interpreted from this analysis, and provides the corresponding limits on $\sqrt{a_1} \Lambda_Q$.

Table 2: Observed and expected allowed intervals at the 95% CL on the H boson average lifetime τ_H and width Γ_H obtained combining the width and lifetime analyses. The constraints are separated into the two conditions used in the width measurement, with either the constraint $f_{\Lambda Q} = 0$, or $f_{\Lambda Q}$ left unconstrained and $\phi_{\Lambda Q} = 0$ or π . The upper (lower) limits on H boson average lifetime τ_H are related to the lower (upper) limits on H boson width Γ_H through Eq. (2).

Parameter	$f_{\Lambda Q} = 0$		$f_{\Lambda Q}$ unconstrained, $\phi_{\Lambda Q} = 0$ or π	
	Observed	Expected	Observed	Expected
τ_H (fs)	$[2.5 \times 10^{-8}, 190]$	$[1.6 \times 10^{-8}, 190]$	$[1.4 \times 10^{-8}, 190]$	$[9 \times 10^{-9}, 190]$
Γ_H (MeV)	$[3.5 \times 10^{-9}, 26]$	$[3.6 \times 10^{-9}, 41]$	$[3.5 \times 10^{-9}, 46]$	$[3.6 \times 10^{-9}, 73]$

Table 3: Observed and expected allowed intervals at the 95% CL on the $f_{\Lambda Q}$ on-shell effective cross-section fraction and its interpretation in terms of the anomalous coupling parameter Λ_Q assuming $\Gamma_H = \Gamma_H^{\text{SM}}$. Results are presented assuming either $\phi_{\Lambda Q} = 0$ or $\phi_{\Lambda Q} = \pi$. The allowed intervals on $f_{\Lambda Q}$ are also translated to the equivalent quantity $\sqrt{a_1} \Lambda_Q$ through Eq. (5), where the coefficient a_1 is allowed to be different from its SM value $a_1 = 2$.

Parameter	$\phi_{\Lambda Q} = 0$		$\phi_{\Lambda Q} = \pi$	
	Observed	Expected	Observed	Expected
$f_{\Lambda Q}$	$< 3.8 \times 10^{-3}$	$< 4.4 \times 10^{-3}$	$< 2.4 \times 10^{-3}$	$< 3.6 \times 10^{-3}$
$\sqrt{a_1} \Lambda_Q$ (GeV)	> 500	> 490	> 570	> 510

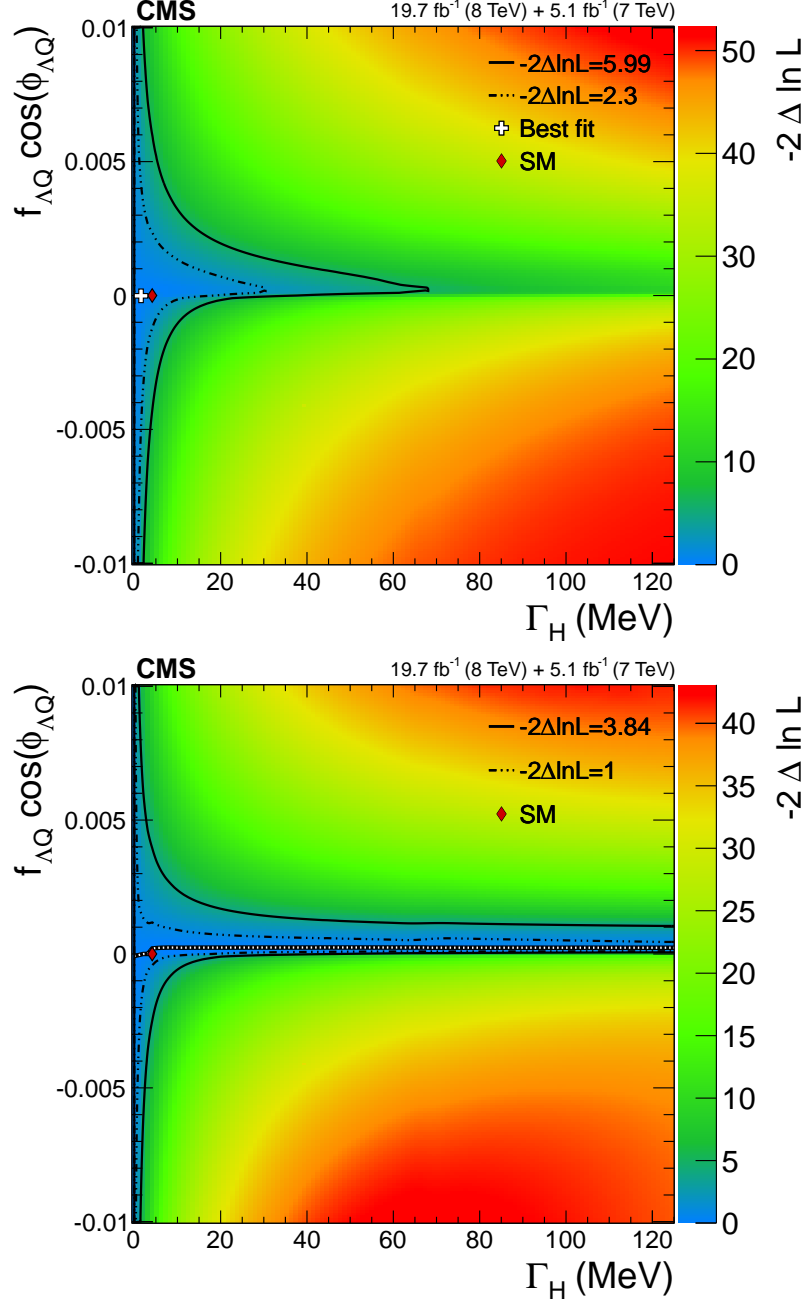


Figure 8: Observed distribution of $-2 \ln(\mathcal{L}/\mathcal{L}_{\max})$ as a function of Γ_H and $f_{\Lambda Q} \cos \phi_{\Lambda Q}$ with the assumption $\phi_{\Lambda Q} = 0$ or π (top panel). The bottom panel shows the observed conditional likelihood scan as a function of $f_{\Lambda Q} \cos \phi_{\Lambda Q}$ for a given Γ_H . The likelihood contours are shown for the two-parameter 68% and 95% CL_s (top) and for the one-parameter 68% and 95% CL_s (bottom). The black curve with white dots on the bottom panel shows the $f_{\Lambda Q} \cos \phi_{\Lambda Q}$ minima at each Γ_H value.

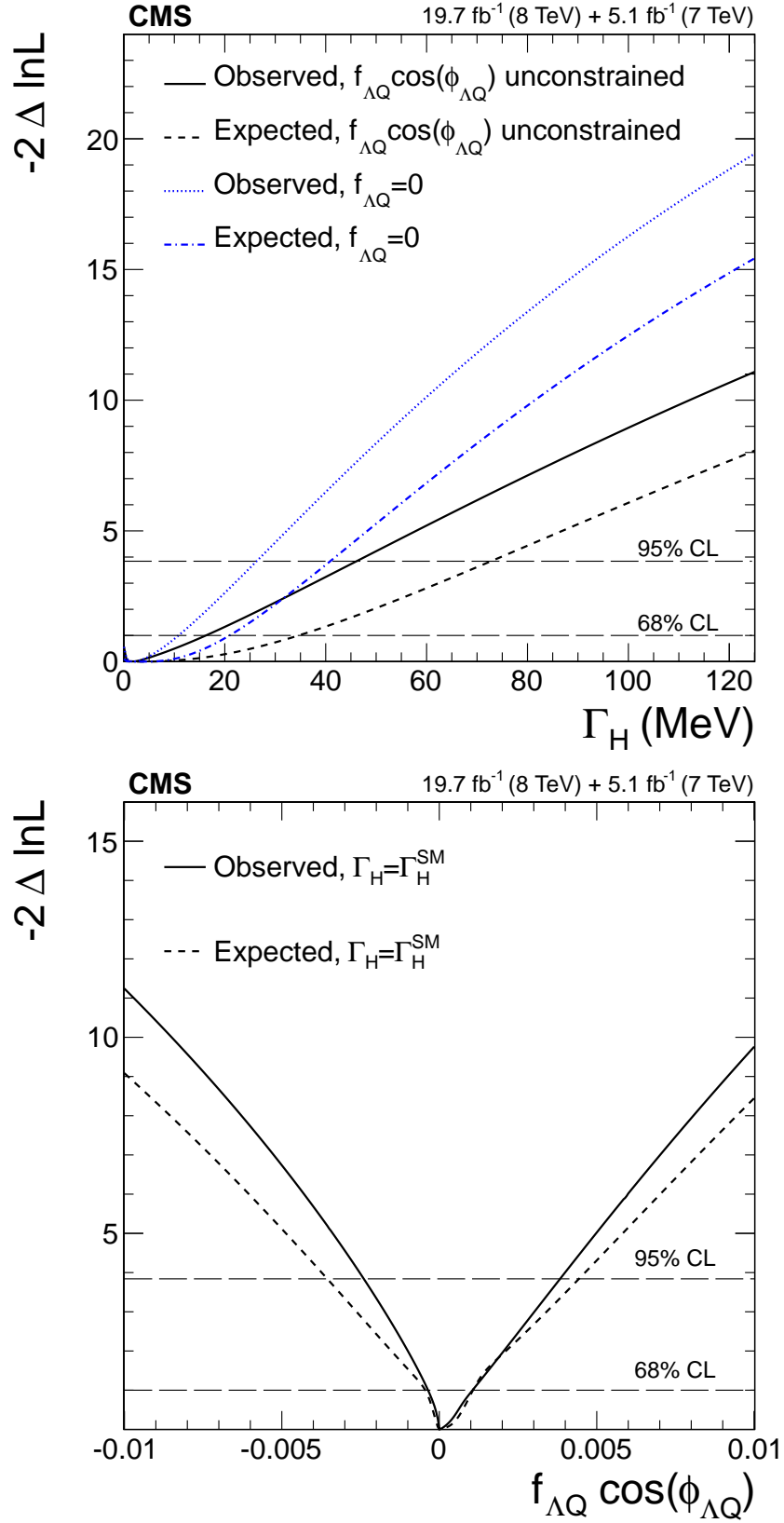


Figure 9: Observed (solid) and expected (dashed) distributions of $-2 \ln(\mathcal{L}/\mathcal{L}_{\max})$ as a function of Γ_H (top) and $f_{\Lambda Q} \cos \phi_{\Lambda Q}$ (bottom). On the top panel, the $f_{\Lambda Q}$ value is either constrained to zero (blue) or left unconstrained (black, weaker limit), while $\Gamma_H = \Gamma_H^{\text{SM}}$ and $\phi_{\Lambda Q} = 0$ or π are assumed on the bottom.

Acknowledgments

We thank Markus Schulze for optimizing the JHUGEN Monte Carlo simulation program and matrix element library for this analysis. We congratulate our colleagues in the CERN accelerator departments for the excellent performance of the LHC and thank the technical and administrative staffs at CERN and at other CMS institutes for their contributions to the success of the CMS effort. In addition, we gratefully acknowledge the computing centers and personnel of the Worldwide LHC Computing Grid for delivering so effectively the computing infrastructure essential to our analyses. Finally, we acknowledge the enduring support for the construction and operation of the LHC and the CMS detector provided by the following funding agencies: the Austrian Federal Ministry of Science, Research and Economy and the Austrian Science Fund; the Belgian Fonds de la Recherche Scientifique, and Fonds voor Wetenschappelijk Onderzoek; the Brazilian funding agencies (CNPq, CAPES, FAPERJ, and FAPESP); the Bulgarian Ministry of Education and Science; CERN; the Chinese Academy of Sciences, Ministry of Science and Technology, and National Natural Science Foundation of China; the Colombian Funding Agency (COLCIENCIAS); the Croatian Ministry of Science, Education and Sport, and the Croatian Science Foundation; the Research Promotion Foundation, Cyprus; the Ministry of Education and Research, Estonian Research Council via IUT23-4 and IUT23-6 and European Regional Development Fund, Estonia; the Academy of Finland, Finnish Ministry of Education and Culture, and Helsinki Institute of Physics; the Institut National de Physique Nucléaire et de Physique des Particules / CNRS, and Commissariat à l'Énergie Atomique et aux Énergies Alternatives / CEA, France; the Bundesministerium für Bildung und Forschung, Deutsche Forschungsgemeinschaft, and Helmholtz-Gemeinschaft Deutscher Forschungszentren, Germany; the General Secretariat for Research and Technology, Greece; the National Scientific Research Foundation, and National Innovation Office, Hungary; the Department of Atomic Energy and the Department of Science and Technology, India; the Institute for Studies in Theoretical Physics and Mathematics, Iran; the Science Foundation, Ireland; the Istituto Nazionale di Fisica Nucleare, Italy; the Ministry of Science, ICT and Future Planning, and National Research Foundation (NRF), Republic of Korea; the Lithuanian Academy of Sciences; the Ministry of Education, and University of Malaya (Malaysia); the Mexican Funding Agencies (CINVESTAV, CONACYT, SEP, and UASLP-FAI); the Ministry of Business, Innovation and Employment, New Zealand; the Pakistan Atomic Energy Commission; the Ministry of Science and Higher Education and the National Science Centre, Poland; the Fundação para a Ciência e a Tecnologia, Portugal; JINR, Dubna; the Ministry of Education and Science of the Russian Federation, the Federal Agency of Atomic Energy of the Russian Federation, Russian Academy of Sciences, and the Russian Foundation for Basic Research; the Ministry of Education, Science and Technological Development of Serbia; the Secretaría de Estado de Investigación, Desarrollo e Innovación and Programa Consolider-Ingenio 2010, Spain; the Swiss Funding Agencies (ETH Board, ETH Zurich, PSI, SNF, UniZH, Canton Zurich, and SER); the Ministry of Science and Technology, Taipei; the Thailand Center of Excellence in Physics, the Institute for the Promotion of Teaching Science and Technology of Thailand, Special Task Force for Activating Research and the National Science and Technology Development Agency of Thailand; the Scientific and Technical Research Council of Turkey, and Turkish Atomic Energy Authority; the National Academy of Sciences of Ukraine, and State Fund for Fundamental Researches, Ukraine; the Science and Technology Facilities Council, UK; the U.S. Department of Energy, and the U.S. National Science Foundation.

Individuals have received support from the Marie Curie program and the European Research Council and EPLANET (European Union); the Leventis Foundation; the A. P. Sloan Foundation; the Alexander von Humboldt Foundation; the Belgian Federal Science Policy Office; the

Fonds pour la Formation à la Recherche dans l'Industrie et dans l'Agriculture (FRIA-Belgium); the Agentschap voor Innovatie door Wetenschap en Technologie (IWT-Belgium); the Ministry of Education, Youth and Sports (MEYS) of the Czech Republic; the Council of Science and Industrial Research, India; the HOMING PLUS program of the Foundation for Polish Science, cofinanced from European Union, Regional Development Fund; the Compagnia di San Paolo (Torino); the Consorzio per la Fisica (Trieste); MIUR project 20108T4XTM (Italy); the Thalís and Aristeia programs cofinanced by EU-ESF and the Greek NSRF; the National Priorities Research Program by Qatar National Research Fund; the Rachadapisek Sompot Fund for Postdoctoral Fellowship, Chulalongkorn University (Thailand); and the Welch Foundation.

References

- [1] ATLAS Collaboration, "Observation of a new particle in the search for the Standard Model Higgs boson with the ATLAS detector at the LHC", *Phys. Lett. B* **716** (2012) 1, doi:10.1016/j.physletb.2012.08.020, arXiv:1207.7214.
- [2] CMS Collaboration, "Observation of a new boson at a mass of 125 GeV with the CMS experiment at the LHC", *Phys. Lett. B* **716** (2012) 30, doi:10.1016/j.physletb.2012.08.021, arXiv:1207.7235.
- [3] CMS Collaboration, "Observation of a new boson with mass near 125 GeV in pp collisions at $\sqrt{s} = 7$ and 8 TeV", *JHEP* **06** (2013) 081, doi:10.1007/JHEP06(2013)081, arXiv:1303.4571.
- [4] F. Englert and R. Brout, "Broken Symmetry and the Mass of Gauge Vector Mesons", *Phys. Rev. Lett.* **13** (1964) 321, doi:10.1103/PhysRevLett.13.321.
- [5] P. W. Higgs, "Broken Symmetries and the Masses of Gauge Bosons", *Phys. Rev. Lett.* **13** (1964) 508, doi:10.1103/PhysRevLett.13.508.
- [6] G. S. Guralnik, C. R. Hagen, and T. W. B. Kibble, "Global Conservation Laws and Massless Particles", *Phys. Rev. Lett.* **13** (1964) 585, doi:10.1103/PhysRevLett.13.585.
- [7] S. L. Glashow, "Partial-symmetries of weak interactions", *Nucl. Phys.* **22** (1961) 579, doi:10.1016/0029-5582(61)90469-2.
- [8] S. Weinberg, "A Model of Leptons", *Phys. Rev. Lett.* **19** (1967) 1264, doi:10.1103/PhysRevLett.19.1264.
- [9] A. Salam, "Weak and electromagnetic interactions", in *Elementary particle physics: relativistic groups and analyticity*, N. Svartholm, ed., p. 367. Almqvist & Wiksell, Stockholm, 1968. Proceedings of the eighth Nobel symposium.
- [10] CMS Collaboration, "Constraints on the Higgs boson width from off-shell production and decay to Z-boson pairs", *Phys. Lett. B* **736** (2014) 64, doi:10.1016/j.physletb.2014.06.077, arXiv:1405.3455.
- [11] ATLAS Collaboration, "Determination of the off-shell Higgs boson signal strength in the high-mass ZZ and WW final states with the ATLAS detector", (2015). arXiv:1503.01060. submitted to Eur. Phys. J. C.

- [12] CMS Collaboration, "Precise determination of the mass of the Higgs boson and tests of compatibility of its couplings with the standard model predictions using proton collisions at 7 and 8 TeV", *Eur. Phys. J. C* **75** (2015) 212, doi:10.1140/epjc/s10052-015-3351-7, arXiv:1412.8662.
- [13] ATLAS Collaboration, "Measurement of the Higgs boson mass from the $H \rightarrow \gamma\gamma$ and $H \rightarrow ZZ^* \rightarrow 4\ell$ channels in pp collisions at center-of-mass energies of 7 and 8 TeV with the ATLAS detector", *Phys. Rev. D* **90** (2014) 052004, doi:10.1103/PhysRevD.90.052004, arXiv:1406.3827.
- [14] CMS Collaboration, "Study of the Mass and Spin-Parity of the Higgs Boson Candidate via Its Decays to Z Boson Pairs", *Phys. Rev. Lett.* **110** (2013) 081803, doi:10.1103/PhysRevLett.110.081803, arXiv:1212.6639.
- [15] ATLAS Collaboration, "Evidence for the spin-0 nature of the Higgs boson using ATLAS data", *Phys. Lett. B* **726** (2013) 120, doi:10.1016/j.physletb.2013.08.026, arXiv:1307.1432.
- [16] CMS Collaboration, "Measurement of the properties of a Higgs boson in the four-lepton final state", *Phys. Rev. D* **89** (2014) 092007, doi:10.1103/PhysRevD.89.092007, arXiv:1312.5353.
- [17] CMS Collaboration, "Constraints on the spin-parity and anomalous HVV couplings of the Higgs boson in proton collisions at 7 and 8 TeV", (2014). arXiv:1411.3441. accepted by Phys. Rev. D.
- [18] ATLAS Collaboration, "Determination of spin and parity of the Higgs boson in the $WW^* \rightarrow e\nu\mu\nu$ decay channel with the ATLAS detector", *Eur. Phys. J. C* **75** (2015) 231, doi:10.1140/epjc/s10052-015-3436-3, arXiv:1503.03643.
- [19] CMS Collaboration, "The CMS experiment at the CERN LHC", *JINST* **3** (2008) S08004, doi:10.1088/1748-0221/3/08/S08004.
- [20] CMS Collaboration, "Search for a Higgs boson in the mass range from 145 to 1000 GeV decaying to a pair of W or Z bosons", (2015). arXiv:1504.00936. submitted to JHEP.
- [21] ATLAS Collaboration, "Measurements of Higgs boson production and couplings in diboson final states with the ATLAS detector at the LHC", *Phys. Lett. B* **726** (2013) 119, doi:10.1016/j.physletb.2013.08.010, arXiv:1307.1427.
- [22] F. Caola and K. Melnikov, "Constraining the Higgs boson width with ZZ production at the LHC", *Phys. Rev. D* **88** (2013) 054024, doi:10.1103/PhysRevD.88.054024, arXiv:1307.4935.
- [23] N. Kauer and G. Passarino, "Inadequacy of zero-width approximation for a light Higgs boson signal", *JHEP* **08** (2012) 116, doi:10.1007/JHEP08(2012)116, arXiv:1206.4803.
- [24] J. M. Campbell, R. K. Ellis, and C. Williams, "Bounding the Higgs width at the LHC using full analytic results for $gg \rightarrow e^-e^+\mu^-\mu^+$ ", *JHEP* **04** (2014) 060, doi:10.1007/JHEP04(2014)060, arXiv:1311.3589.
- [25] J. S. Gainer et al., "Beyond geolocating: Constraining higher dimensional operators in $H \rightarrow 4\ell$ with off-shell production and more", *Phys. Rev. D* **91** (2015) 035011, doi:10.1103/PhysRevD.91.035011, arXiv:1403.4951.

- [26] C. Englert and M. Spannowsky, “Limitations and opportunities of off-shell coupling measurements”, *Phys. Rev. D* **90** (2014) 053003, doi:10.1103/PhysRevD.90.053003, arXiv:1405.0285.
- [27] M. Ghezzi, G. Passarino, and S. Uccirati, “Bounding the Higgs Width Using Effective Field Theory”, (2014). arXiv:1405.1925.
- [28] CMS Collaboration, “Absolute Calibration of the Luminosity Measurement at CMS: Winter 2012 Update”, Report No. CMS-PAS-SMP-12-008, 2012.
- [29] CMS Collaboration, “CMS Luminosity Based on Pixel Cluster Counting - Summer 2013 Update”, Report No. CMS-PAS-LUM-13-001, 2013.
- [30] LHC Higgs Cross Section Working Group, “Handbook of LHC Higgs Cross Sections: 1. Inclusive Observables”, CERN Report CERN-2011-002, 2011. arXiv:1101.0593.
- [31] LHC Higgs Cross Section Working Group, “Handbook of LHC Higgs Cross Sections: 3. Higgs Properties”, CERN Report CERN-2013-004, 2013. doi:10.5170/CERN-2013-004, arXiv:1307.1347.
- [32] S. Frixione, P. Nason, and C. Oleari, “Matching NLO QCD computations with parton shower simulations: the POWHEG method”, *JHEP* **11** (2007) 070, doi:10.1088/1126-6708/2007/11/070, arXiv:0709.2092.
- [33] E. Bagnaschi, G. Degrandi, P. Slavich, and A. Vicini, “Higgs production via gluon fusion in the POWHEG approach in the SM and in the MSSM”, *JHEP* **02** (2012) 088, doi:10.1007/JHEP02(2012)088, arXiv:1111.2854.
- [34] P. Nason and C. Oleari, “NLO Higgs boson production via vector-boson fusion matched with shower in POWHEG”, *JHEP* **02** (2010) 037, doi:10.1007/JHEP02(2010)037, arXiv:0911.5299.
- [35] Y. Gao et al., “Spin determination of single-produced resonances at hadron colliders”, *Phys. Rev. D* **81** (2010) 075022, doi:10.1103/PhysRevD.81.075022, arXiv:1001.3396. [Erratum: doi:10.1103/PhysRevD.81.079905].
- [36] S. Bolognesi et al., “On the spin and parity of a single-produced resonance at the LHC”, *Phys. Rev. D* **86** (2012) 095031, doi:10.1103/PhysRevD.86.095031, arXiv:1208.4018.
- [37] I. Anderson et al., “Constraining anomalous HVV interactions at proton and lepton colliders”, *Phys. Rev. D* **89** (2014) 035007, doi:10.1103/PhysRevD.89.035007, arXiv:1309.4819.
- [38] J. M. Campbell et al., “NLO Higgs boson production plus one and two jets using the POWHEG BOX, MadGraph4 and MCFM”, *JHEP* **07** (2012) 092, doi:10.1007/JHEP07(2012)092, arXiv:1202.5475.
- [39] K. Hamilton, P. Nason, and G. Zanderighi, “MINLO: multi-scale improved NLO”, *JHEP* **10** (2012) 155, doi:10.1007/JHEP10(2012)155, arXiv:1206.3572.
- [40] T. Sjöstrand, S. Mrenna, and P. Skands, “PYTHIA 6.4 physics and manual”, *JHEP* **05** (2006) 026, doi:10.1088/1126-6708/2006/05/026, arXiv:hep-ph/0603175.

- [41] J. M. Campbell and R. K. Ellis, “MCFM for the Tevatron and the LHC”, *Nucl. Phys. Proc. Suppl.* **205** (2010) 10, doi:10.1016/j.nuclphysbps.2010.08.011, arXiv:1007.3492.
- [42] J. M. Campbell, R. K. Ellis, and C. Williams, “Vector boson pair production at the LHC”, *JHEP* **07** (2011) 018, doi:10.1007/JHEP07(2011)018, arXiv:1105.0020.
- [43] T. Binoth, N. Kauer, and P. Mertsch, “Gluon-induced QCD corrections to $pp \rightarrow ZZ \rightarrow \ell\bar{\ell}\ell'\bar{\ell}'$ ”, (2008). arXiv:0807.0024.
- [44] A. Ballestrero et al., “PHANTOM: a Monte Carlo event generator for six parton final states at high energy colliders”, *Comput. Phys. Commun.* **180** (2009) 401, doi:10.1016/j.cpc.2008.10.005, arXiv:0801.3359.
- [45] Particle Data Group, K. A. Olive et al., “Review of Particle Physics”, *Chin. Phys. C* **38** (2014) 090001, doi:10.1088/1674-1137/38/9/090001.
- [46] G. Passarino, “Higgs CAT”, *Eur. Phys. J. C* **74** (2014) 2866, doi:10.1140/epjc/s10052-014-2866-7, arXiv:1312.2397.
- [47] M. Bonvini et al., “Signal-background interference effects in $gg \rightarrow H \rightarrow WW$ beyond leading order”, *Phys. Rev. D* **88** (2013) 034032, doi:10.1103/PhysRevD.88.034032, arXiv:1304.3053.
- [48] K. Melnikov and M. Dowling, “Production of two Z-bosons in gluon fusion in the heavy top quark approximation”, *Phys. Lett. B* **744** (2015) 43, doi:10.1016/j.physletb.2015.03.030, arXiv:1503.01274.
- [49] C. S. Li, H. T. Li, D. Y. Shao, and J. Wang, “Soft gluon resummation in the signal-background interference process of $gg(\rightarrow h^*) \rightarrow ZZ$ ”, (2015). arXiv:1504.02388.
- [50] O. Brein, R. V. Harlander, M. Wieseman, and T. Zirke, “Top-quark mediated effects in hadronic Higgs-Strahlung”, *Eur. Phys. J. C* **72** (2012) 1868, doi:10.1140/epjc/s10052-012-1868-6, arXiv:1111.0761.
- [51] A. Bierweiler, T. Kasprzik, and J. H. Kühn, “Vector-boson pair production at the LHC to $\mathcal{O}(\alpha^3)$ accuracy”, *JHEP* **12** (2013) 071, doi:10.1007/JHEP12(2013)071, arXiv:1305.5402.
- [52] J. Baglio, L. D. Ninh, and M. M. Weber, “Massive gauge boson pair production at LHC: a next-to-leading order story”, *Phys. Rev. D* **88** (2013) 113005, doi:10.1103/PhysRevD.88.113005, arXiv:1307.4331.
- [53] J. Alwall et al., “MadGraph/MadEvent v4: the new web generation”, *JHEP* **09** (2007) 028, doi:10.1088/1126-6708/2007/09/028, arXiv:0706.2334.
- [54] GEANT4 Collaboration, “GEANT4—a simulation toolkit”, *Nucl. Instrum. Meth. A* **506** (2003) 250, doi:10.1016/S0168-9002(03)01368-8.
- [55] CMS Collaboration, “Performance of electron reconstruction and selection with the CMS detector in proton-proton collisions at $\sqrt{s} = 8$ TeV”, *JINST* **10** (2015) P06005, doi:10.1088/1748-0221/10/06/P06005, arXiv:1502.02701.

- [56] CMS Collaboration, “Performance of CMS muon reconstruction in pp collision events at $\sqrt{s} = 7$ TeV”, *JINST* **7** (2012) P10002, doi:10.1088/1748-0221/7/10/P10002, arXiv:1206.4071.
- [57] CMS Collaboration, “Search for long-lived particles that decay into final states containing two electrons or two muons in proton-proton collisions at $\sqrt{s} = 8$ TeV”, *Phys. Rev. D* **91** (2015) 052012, doi:10.1103/PhysRevD.91.052012, arXiv:1411.6977.
- [58] CMS Collaboration, “Search for Displaced Supersymmetry in Events with an Electron and a Muon with Large Impact Parameters”, *Phys. Rev. Lett.* **114** (2015) 061801, doi:10.1103/PhysRevLett.114.061801, arXiv:1409.4789.
- [59] CMS Collaboration, “Description and performance of track and primary-vertex reconstruction with the CMS tracker”, *JINST* **9** (2014) P10009, doi:10.1088/1748-0221/9/10/P10009, arXiv:1405.6569.
- [60] CMS Collaboration, “Particle-Flow Event Reconstruction in CMS and Performance for Jets, Taus, and MET”, Report No. CMS-PAS-PFT-09-001, 2009.
- [61] CMS Collaboration, “Commissioning of the Particle-flow Event Reconstruction with the first LHC collisions recorded in the CMS detector”, Report No. CMS-PAS-PFT-10-001, 2010.
- [62] CMS Collaboration, “Commissioning of the Particle-Flow reconstruction in Minimum-Bias and Jet Events from pp Collisions at 7 TeV”, Report No. CMS-PAS-PFT-10-002, 2010.
- [63] CMS Collaboration, “Commissioning of the particle-flow event reconstruction with leptons from J/ψ and W decays at 7 TeV”, Report No. CMS-PAS-PFT-10-003, 2010.
- [64] M. Cacciari, G. P. Salam, and G. Soyez, “The anti- k_t jet clustering algorithm”, *JHEP* **04** (2008) 063, doi:10.1088/1126-6708/2008/04/063, arXiv:0802.1189.
- [65] M. Cacciari, G. P. Salam, and G. Soyez, “FastJet user manual”, *Eur. Phys. J. C* **72** (2012) 1896, doi:10.1140/epjc/s10052-012-1896-2, arXiv:1111.6097.
- [66] M. Cacciari and G. P. Salam, “Dispelling the N^3 myth for the k_t jet-finder”, *Phys. Lett. B* **641** (2006) 57, doi:10.1016/j.physletb.2006.08.037, arXiv:hep-ph/0512210.
- [67] CMS Collaboration, “Determination of jet energy calibration and transverse momentum resolution in CMS”, *JINST* **6** (2011) P11002, doi:10.1088/1748-0221/6/11/P11002, arXiv:1107.4277.
- [68] M. Cacciari and G. P. Salam, “Pileup subtraction using jet areas”, *Phys. Lett. B* **659** (2008) 119, doi:10.1016/j.physletb.2007.09.077, arXiv:0707.1378.
- [69] M. Cacciari, G. P. Salam, and G. Soyez, “The catchment area of jets”, *JHEP* **04** (2008) 005, doi:10.1088/1126-6708/2008/04/005, arXiv:0802.1188.
- [70] CMS Collaboration, “Pileup Jet Identification”, Report No. CMS-PAS-JME-13-005, 2013.
- [71] CMS Collaboration, “Evidence for the 125 GeV Higgs boson decaying to a pair of τ leptons”, *JHEP* **05** (2014) 104, doi:10.1007/JHEP05(2014)104, arXiv:1401.5041.
- [72] S. S. Wilks, “The Large-Sample Distribution of the Likelihood Ratio for Testing Composite Hypotheses”, *Ann. Math. Stat.* **9** (1938) 60, doi:10.1214/aoms/1177732360.

A The CMS Collaboration

Yerevan Physics Institute, Yerevan, Armenia

V. Khachatryan, A.M. Sirunyan, A. Tumasyan

Institut für Hochenergiephysik der OeAW, Wien, Austria

W. Adam, E. Asilar, T. Bergauer, J. Brandstetter, E. Brondolin, M. Dragicevic, J. Erö, M. Flechl, M. Friedl, R. Frühwirth¹, V.M. Ghete, C. Hartl, N. Hörmann, J. Hrubec, M. Jeitler¹, V. Knünz, A. König, M. Krammer¹, I. Krätschmer, D. Liko, T. Matsushita, I. Mikulec, D. Rabady², B. Rahbaran, H. Rohringer, J. Schieck¹, R. Schöfbeck, J. Strauss, W. Treberer-Treberspurg, W. Waltenberger, C.-E. Wulz¹

National Centre for Particle and High Energy Physics, Minsk, Belarus

V. Mossolov, N. Shumeiko, J. Suarez Gonzalez

Universiteit Antwerpen, Antwerpen, Belgium

S. Alderweireldt, T. Cornelis, E.A. De Wolf, X. Janssen, A. Knutsson, J. Lauwers, S. Luyckx, S. Ochesanu, R. Rougny, M. Van De Klundert, H. Van Haevermaet, P. Van Mechelen, N. Van Remortel, A. Van Spilbeeck

Vrije Universiteit Brussel, Brussel, Belgium

S. Abu Zeid, F. Blekman, J. D'Hondt, N. Daci, I. De Bruyn, K. Deroover, N. Heracleous, J. Keaveney, S. Lowette, L. Moreels, A. Olbrechts, Q. Python, D. Strom, S. Tavernier, W. Van Doninck, P. Van Mulders, G.P. Van Onsem, I. Van Parijs

Université Libre de Bruxelles, Bruxelles, Belgium

P. Barria, C. Caillol, B. Clerboux, G. De Lentdecker, H. Delannoy, G. Fasanella, L. Favart, A.P.R. Gay, A. Grebenyuk, T. Lenzi, A. Léonard, T. Maerschalk, A. Marinov, L. Perniè, A. Randle-conde, T. Reis, T. Seva, C. Vander Velde, P. Vanlaer, R. Yonamine, F. Zenoni, F. Zhang³

Ghent University, Ghent, Belgium

K. Beernaert, L. Benucci, A. Cimmino, S. Crucy, D. Dobur, A. Fagot, G. Garcia, M. Gul, J. Mccartin, A.A. Ocampo Rios, D. Poyraz, D. Ryckbosch, S. Salva, M. Sigamani, N. Strobbe, M. Tytgat, W. Van Driessche, E. Yazgan, N. Zaganidis

Université Catholique de Louvain, Louvain-la-Neuve, Belgium

S. Basegmez, C. Beluffi⁴, O. Bondu, S. Brochet, G. Bruno, R. Castello, A. Caudron, L. Ceard, G.G. Da Silveira, C. Delaere, D. Favart, L. Forthomme, A. Giammanco⁵, J. Hollar, A. Jafari, P. Jez, M. Komm, V. Lemaître, A. Mertens, C. Nuttens, L. Perrini, A. Pin, K. Piotrkowski, A. Popov⁶, L. Quertenmont, M. Selvaggi, M. Vidal Marono

Université de Mons, Mons, Belgium

N. Beliy, G.H. Hammad

Centro Brasileiro de Pesquisas Físicas, Rio de Janeiro, Brazil

W.L. Aldá Júnior, G.A. Alves, L. Brito, M. Correa Martins Junior, M. Hamer, C. Hensel, C. Mora Herrera, A. Moraes, M.E. Pol, P. Rebello Teles

Universidade do Estado do Rio de Janeiro, Rio de Janeiro, Brazil

E. Belchior Batista Das Chagas, W. Carvalho, J. Chinellato⁷, A. Custódio, E.M. Da Costa, D. De Jesus Damiao, C. De Oliveira Martins, S. Fonseca De Souza, L.M. Huertas Guativa, H. Malbouisson, D. Matos Figueiredo, L. Mundim, H. Nogima, W.L. Prado Da Silva, A. Santoro, A. Sznajder, E.J. Tonelli Manganote⁷, A. Vilela Pereira

Universidade Estadual Paulista ^a, Universidade Federal do ABC ^b, São Paulo, Brazil

S. Ahuja^a, C.A. Bernardes^b, A. De Souza Santos^b, S. Dogra^a, T.R. Fernandez Perez Tomei^a, E.M. Gregores^b, P.G. Mercadante^b, C.S. Moon^{a,8}, S.F. Novaes^a, Sandra S. Padula^a, D. Romero Abad, J.C. Ruiz Vargas

Institute for Nuclear Research and Nuclear Energy, Sofia, Bulgaria

A. Aleksandrov, V. Genchev[†], R. Hadjiiska, P. Iaydjiev, S. Piperov, M. Rodozov, S. Stoykova, G. Sultanov, M. Vutova

University of Sofia, Sofia, Bulgaria

A. Dimitrov, I. Glushkov, L. Litov, B. Pavlov, P. Petkov

Institute of High Energy Physics, Beijing, China

M. Ahmad, J.G. Bian, G.M. Chen, H.S. Chen, M. Chen, T. Cheng, R. Du, C.H. Jiang, R. Plestina⁹, F. Romeo, S.M. Shaheen, J. Tao, C. Wang, Z. Wang, H. Zhang

State Key Laboratory of Nuclear Physics and Technology, Peking University, Beijing, China

C. Asawatrangkuldee, Y. Ban, Q. Li, S. Liu, Y. Mao, S.J. Qian, D. Wang, Z. Xu, W. Zou

Universidad de Los Andes, Bogota, Colombia

C. Avila, A. Cabrera, L.F. Chaparro Sierra, C. Florez, J.P. Gomez, B. Gomez Moreno, J.C. Sanabria

University of Split, Faculty of Electrical Engineering, Mechanical Engineering and Naval Architecture, Split, Croatia

N. Godinovic, D. Lelas, D. Polic, I. Puljak, P.M. Ribeiro Cipriano

University of Split, Faculty of Science, Split, Croatia

Z. Antunovic, M. Kovac

Institute Rudjer Boskovic, Zagreb, Croatia

V. Brigljevic, K. Kadija, J. Luetic, S. Micanovic, L. Sudic

University of Cyprus, Nicosia, Cyprus

A. Attikis, G. Mavromanolakis, J. Mousa, C. Nicolaou, F. Ptochos, P.A. Razis, H. Rykaczewski

Charles University, Prague, Czech Republic

M. Bodlak, M. Finger¹⁰, M. Finger Jr.¹⁰

Academy of Scientific Research and Technology of the Arab Republic of Egypt, Egyptian Network of High Energy Physics, Cairo, Egypt

E. El-khateeb¹¹, T. Elkafrawy¹¹, A. Mohamed¹², E. Salama^{11,13}

National Institute of Chemical Physics and Biophysics, Tallinn, Estonia

B. Calpas, M. Kadastik, M. Murumaa, M. Raidal, A. Tiko, C. Veelken

Department of Physics, University of Helsinki, Helsinki, Finland

P. Eerola, J. Pekkanen, M. Voutilainen

Helsinki Institute of Physics, Helsinki, Finland

J. Härkönen, V. Karimäki, R. Kinnunen, T. Lampén, K. Lassila-Perini, S. Lehti, T. Lindén, P. Luukka, T. Mäenpää, T. Peltola, E. Tuominen, J. Tuominiemi, E. Tuovinen, L. Wendland

Lappeenranta University of Technology, Lappeenranta, Finland

J. Talvitie, T. Tuuva

DSM/IRFU, CEA/Saclay, Gif-sur-Yvette, France

M. Besancon, F. Couderc, M. Dejardin, D. Denegri, B. Fabbro, J.L. Faure, C. Favaro, F. Ferri, S. Ganjour, A. Givernaud, P. Gras, G. Hamel de Monchenault, P. Jarry, E. Locci, M. Machet, J. Malcles, J. Rander, A. Rosowsky, M. Titov, A. Zghiche

Laboratoire Leprince-Ringuet, Ecole Polytechnique, IN2P3-CNRS, Palaiseau, France

I. Antropov, S. Baffioni, F. Beaudette, P. Busson, L. Cadamuro, E. Chapon, C. Charlot, T. Dahms, O. Davignon, N. Filipovic, A. Florent, R. Granier de Cassagnac, S. Lisniak, L. Mastrolorenzo, P. Miné, I.N. Naranjo, M. Nguyen, C. Ochando, G. Ortona, P. Paganini, S. Regnard, R. Salerno, J.B. Sauvan, Y. Sirois, T. Strebler, Y. Yilmaz, A. Zabi

Institut Pluridisciplinaire Hubert Curien, Université de Strasbourg, Université de Haute Alsace Mulhouse, CNRS/IN2P3, Strasbourg, France

J.-L. Agram¹⁴, J. Andrea, A. Aubin, D. Bloch, J.-M. Brom, M. Buttignol, E.C. Chabert, N. Chanon, C. Collard, E. Conte¹⁴, X. Coubez, J.-C. Fontaine¹⁴, D. Gelé, U. Goerlach, C. Goetzmann, A.-C. Le Bihan, J.A. Merlin², K. Skovpen, P. Van Hove

Centre de Calcul de l'Institut National de Physique Nucleaire et de Physique des Particules, CNRS/IN2P3, Villeurbanne, France

S. Gadrat

Université de Lyon, Université Claude Bernard Lyon 1, CNRS-IN2P3, Institut de Physique Nucléaire de Lyon, Villeurbanne, France

S. Beauceron, C. Bernet, G. Boudoul, E. Bouvier, C.A. Carrillo Montoya, J. Chasserat, R. Chierici, D. Contardo, B. Courbon, P. Depasse, H. El Mamouni, J. Fan, J. Fay, S. Gascon, M. Gouzevitch, B. Ille, F. Lagarde, I.B. Laktineh, M. Lethuillier, L. Mirabito, A.L. Pequegnot, S. Perries, J.D. Ruiz Alvarez, D. Sabes, L. Sgandurra, V. Sordini, M. Vander Donckt, P. Verdier, S. Viret, H. Xiao

Georgian Technical University, Tbilisi, Georgia

T. Toriashvili¹⁵

Tbilisi State University, Tbilisi, Georgia

Z. Tsamalaidze¹⁰

RWTH Aachen University, I. Physikalisches Institut, Aachen, Germany

C. Autermann, S. Beranek, M. Edelhoff, L. Feld, A. Heister, M.K. Kiesel, K. Klein, M. Lipinski, A. Ostapchuk, M. Preuten, F. Raupach, S. Schael, J.F. Schulte, T. Verlage, H. Weber, B. Wittmer, V. Zhukov⁶

RWTH Aachen University, III. Physikalisches Institut A, Aachen, Germany

M. Ata, M. Brodski, E. Dietz-Laursonn, D. Duchardt, M. Endres, M. Erdmann, S. Erdweg, T. Esch, R. Fischer, A. Güth, T. Hebbeker, C. Heidemann, K. Hoepfner, D. Klingebiel, S. Knutzen, P. Kreuzer, M. Merschmeyer, A. Meyer, P. Millet, M. Olschewski, K. Padeken, P. Papacz, T. Pook, M. Radziej, H. Reithler, M. Rieger, F. Scheuch, L. Sonnenschein, D. Teyssier, S. Thüer

RWTH Aachen University, III. Physikalisches Institut B, Aachen, Germany

V. Cherepanov, Y. Erdogan, G. Flügge, H. Geenen, M. Geisler, F. Hoehle, B. Kargoll, T. Kress, Y. Kuessel, A. Künsken, J. Lingemann², A. Nehr Korn, A. Nowack, I.M. Nugent, C. Pistone, O. Pooth, A. Stahl

Deutsches Elektronen-Synchrotron, Hamburg, Germany

M. Aldaya Martin, I. Asin, N. Bartosik, O. Behnke, U. Behrens, A.J. Bell, K. Borras, A. Burgmeier, A. Cakir, L. Calligaris, A. Campbell, S. Choudhury, F. Costanza, C. Diez

Pardos, G. Dolinska, S. Dooling, T. Dorland, G. Eckerlin, D. Eckstein, T. Eichhorn, G. Flucke, E. Gallo, J. Garay Garcia, A. Geiser, A. Gizhko, P. Gunnellini, J. Hauk, M. Hempel¹⁶, H. Jung, A. Kalogeropoulos, O. Karacheban¹⁶, M. Kasemann, P. Katsas, J. Kieseler, C. Kleinwort, I. Korol, W. Lange, J. Leonard, K. Lipka, A. Lobanov, W. Lohmann¹⁶, R. Mankel, I. Marfin¹⁶, I.-A. Melzer-Pellmann, A.B. Meyer, G. Mittag, J. Mnich, A. Mussgiller, S. Naumann-Emme, A. Nayak, E. Ntomari, H. Perrey, D. Pitzl, R. Placakyte, A. Raspereza, B. Roland, M.Ö. Sahin, P. Saxena, T. Schoerner-Sadenius, M. Schröder, C. Seitz, S. Spannagel, K.D. Trippkewitz, R. Walsh, C. Wissing

University of Hamburg, Hamburg, Germany

V. Blobel, M. Centis Vignali, A.R. Draeger, J. Erfle, E. Garutti, K. Goebel, D. Gonzalez, M. Görner, J. Haller, M. Hoffmann, R.S. Höing, A. Junkes, R. Klanner, R. Kogler, T. Lapsien, T. Lenz, I. Marchesini, D. Marconi, D. Nowatschin, J. Ott, F. Pantaleo², T. Peiffer, A. Perieanu, N. Pietsch, J. Poehlsen, D. Rathjens, C. Sander, H. Schettler, P. Schleper, E. Schlieckau, A. Schmidt, J. Schwandt, M. Seidel, V. Sola, H. Stadie, G. Steinbrück, H. Tholen, D. Troendle, E. Usai, L. Vanelderen, A. Vanhoefer

Institut für Experimentelle Kernphysik, Karlsruhe, Germany

M. Akbiyik, C. Barth, C. Baus, J. Berger, C. Böser, E. Butz, T. Chwalek, F. Colombo, W. De Boer, A. Descroix, A. Dierlamm, S. Fink, F. Frensch, M. Giffels, A. Gilbert, F. Hartmann², S.M. Heindl, U. Husemann, I. Katkov⁶, A. Kornmayer², P. Lobelle Pardo, B. Maier, H. Mildner, M.U. Mozer, T. Müller, Th. Müller, M. Plagge, G. Quast, K. Rabbertz, S. Röcker, F. Roscher, H.J. Simonis, F.M. Stober, R. Ulrich, J. Wagner-Kuhr, S. Wayand, M. Weber, T. Weiler, C. Wöhrmann, R. Wolf

Institute of Nuclear and Particle Physics (INPP), NCSR Demokritos, Aghia Paraskevi, Greece

G. Anagnostou, G. Daskalakis, T. Geralis, V.A. Giakoumopoulou, A. Kyriakis, D. Loukas, A. Psallidas, I. Topsis-Giotis

University of Athens, Athens, Greece

A. Agapitos, S. Kesisoglou, A. Panagiotou, N. Saoulidou, E. Tziaferi

University of Ioánnina, Ioánnina, Greece

I. Evangelou, G. Flouris, C. Foudas, P. Kokkas, N. Loukas, N. Manthos, I. Papadopoulos, E. Paradas, J. Strologas

Wigner Research Centre for Physics, Budapest, Hungary

G. Bencze, C. Hajdu, A. Hazi, P. Hidas, D. Horvath¹⁷, F. Sikler, V. Veszpremi, G. Vesztergombi¹⁸, A.J. Zsigmond

Institute of Nuclear Research ATOMKI, Debrecen, Hungary

N. Beni, S. Czellar, J. Karancsi¹⁹, J. Molnar, Z. Szillasi

University of Debrecen, Debrecen, Hungary

M. Bartók²⁰, A. Makovec, P. Raics, Z.L. Trocsanyi, B. Ujvari

National Institute of Science Education and Research, Bhubaneswar, India

P. Mal, K. Mandal, N. Sahoo, S.K. Swain

Panjab University, Chandigarh, India

S. Bansal, S.B. Beri, V. Bhatnagar, R. Chawla, R. Gupta, U. Bhawandeep, A.K. Kalsi, A. Kaur, M. Kaur, R. Kumar, A. Mehta, M. Mittal, J.B. Singh, G. Walia

University of Delhi, Delhi, India

Ashok Kumar, Arun Kumar, A. Bhardwaj, B.C. Choudhary, R.B. Garg, A. Kumar, S. Malhotra, M. Naimuddin, N. Nishu, K. Ranjan, R. Sharma, V. Sharma

Saha Institute of Nuclear Physics, Kolkata, India

S. Banerjee, S. Bhattacharya, K. Chatterjee, S. Dey, S. Dutta, Sa. Jain, N. Majumdar, A. Modak, K. Mondal, S. Mukherjee, S. Mukhopadhyay, A. Roy, D. Roy, S. Roy Chowdhury, S. Sarkar, M. Sharan

Bhabha Atomic Research Centre, Mumbai, India

A. Abdulsalam, R. Chudasama, D. Dutta, V. Jha, V. Kumar, A.K. Mohanty², L.M. Pant, P. Shukla, A. Topkar

Tata Institute of Fundamental Research, Mumbai, India

T. Aziz, S. Banerjee, S. Bhowmik²¹, R.M. Chatterjee, R.K. Dewanjee, S. Dugad, S. Ganguly, S. Ghosh, M. Guchait, A. Gurtu²², G. Kole, S. Kumar, B. Mahakud, M. Maity²¹, G. Majumder, K. Mazumdar, S. Mitra, G.B. Mohanty, B. Parida, T. Sarkar²¹, K. Sudhakar, N. Sur, B. Sutar, N. Wickramage²³

Indian Institute of Science Education and Research (IISER), Pune, India

S. Chauhan, S. Dube, S. Sharma

Institute for Research in Fundamental Sciences (IPM), Tehran, Iran

H. Bakhshiansohi, H. Behnamian, S.M. Etesami²⁴, A. Fahim²⁵, R. Goldouzian, M. Khakzad, M. Mohammadi Najafabadi, M. Naseri, S. Paktinat Mehdiabadi, F. Rezaei Hosseinabadi, B. Safarzadeh²⁶, M. Zeinali

University College Dublin, Dublin, Ireland

M. Felcini, M. Grunewald

INFN Sezione di Bari ^a, Università di Bari ^b, Politecnico di Bari ^c, Bari, Italy

M. Abbrescia^{a,b}, C. Calabria^{a,b}, C. Caputo^{a,b}, S.S. Chhibra^{a,b}, A. Colaleo^a, D. Creanza^{a,c}, L. Cristella^{a,b}, N. De Filippis^{a,c}, M. De Palma^{a,b}, L. Fiore^a, G. Iaselli^{a,c}, G. Maggi^{a,c}, M. Maggi^a, G. Miniello^{a,b}, S. My^{a,c}, S. Nuzzo^{a,b}, A. Pompili^{a,b}, G. Pugliese^{a,c}, R. Radogna^{a,b}, A. Ranieri^a, G. Selvaggi^{a,b}, L. Silvestris^{a,2}, R. Venditti^{a,b}, P. Verwilligen^a

INFN Sezione di Bologna ^a, Università di Bologna ^b, Bologna, Italy

G. Abbiendi^a, C. Battilana², A.C. Benvenuti^a, D. Bonacorsi^{a,b}, S. Braibant-Giacomelli^{a,b}, L. Brigliadori^{a,b}, R. Campanini^{a,b}, P. Capiluppi^{a,b}, A. Castro^{a,b}, F.R. Cavallo^a, G. Codispoti^{a,b}, M. Cuffiani^{a,b}, G.M. Dallavalle^a, F. Fabbri^a, A. Fanfani^{a,b}, D. Fasanella^{a,b}, P. Giacomelli^a, C. Grandi^a, L. Guiducci^{a,b}, S. Marcellini^a, G. Masetti^a, A. Montanari^a, F.L. Navarria^{a,b}, A. Perrotta^a, A.M. Rossi^{a,b}, T. Rovelli^{a,b}, G.P. Siroli^{a,b}, N. Tosi^{a,b}, R. Travaglini^{a,b}

INFN Sezione di Catania ^a, Università di Catania ^b, CSFNSM ^c, Catania, Italy

G. Cappello^a, M. Chiorboli^{a,b}, S. Costa^{a,b}, F. Giordano^a, R. Potenza^{a,b}, A. Tricomi^{a,b}, C. Tuve^{a,b}

INFN Sezione di Firenze ^a, Università di Firenze ^b, Firenze, Italy

G. Barbagli^a, V. Ciulli^{a,b}, C. Civinini^a, R. D'Alessandro^{a,b}, E. Focardi^{a,b}, S. Gonzi^{a,b}, V. Gori^{a,b}, P. Lenzi^{a,b}, M. Meschini^a, S. Paoletti^a, G. Sguazzoni^a, A. Tropiano^{a,b}, L. Viliani^{a,b}

INFN Laboratori Nazionali di Frascati, Frascati, Italy

L. Benussi, S. Bianco, F. Fabbri, D. Piccolo

INFN Sezione di Genova ^a, Università di Genova ^b, Genova, Italy

V. Calvelli^{a,b}, F. Ferro^a, M. Lo Vetere^{a,b}, M.R. Monge^{a,b}, E. Robutti^a, S. Tosi^{a,b}

INFN Sezione di Milano-Bicocca ^a, Università di Milano-Bicocca ^b, Milano, Italy

L. Brianza, M.E. Dinardo^{a,b}, S. Fiorendi^{a,b}, S. Gennai^a, R. Gerosa^{a,b}, A. Ghezzi^{a,b}, P. Govoni^{a,b}, S. Malvezzi^a, R.A. Manzoni^{a,b}, B. Marzocchi^{a,b,2}, D. Menasce^a, L. Moroni^a, M. Paganoni^{a,b}, D. Pedrini^a, S. Ragazzi^{a,b}, N. Redaelli^a, T. Tabarelli de Fatis^{a,b}

INFN Sezione di Napoli ^a, Università di Napoli 'Federico II' ^b, Napoli, Italy, Università della Basilicata ^c, Potenza, Italy, Università G. Marconi ^d, Roma, Italy

S. Buontempo^a, N. Cavallo^{a,c}, S. Di Guida^{a,d,2}, M. Esposito^{a,b}, F. Fabozzi^{a,c}, A.O.M. Iorio^{a,b}, G. Lanza^a, L. Lista^a, S. Meola^{a,d,2}, M. Merola^a, P. Paolucci^{a,2}, C. Sciacca^{a,b}, F. Thyssen

INFN Sezione di Padova ^a, Università di Padova ^b, Padova, Italy, Università di Trento ^c, Trento, Italy

P. Azzi^{a,2}, N. Bacchetta^a, L. Benato^{a,b}, D. Bisello^{a,b}, A. Boletti^{a,b}, A. Branca^{a,b}, R. Carlin^{a,b}, A. Carvalho Antunes De Oliveira^{a,b}, P. Checchia^a, M. Dall'Osso^{a,b,2}, T. Dorigo^a, U. Dosselli^a, F. Gasparini^{a,b}, U. Gasparini^{a,b}, A. Gozzelino^a, K. Kanishchev^{a,c}, S. Lacaprara^a, M. Margoni^{a,b}, A.T. Meneguzzo^{a,b}, J. Pazzini^{a,b}, N. Pozzobon^{a,b}, P. Ronchese^{a,b}, F. Simonetto^{a,b}, E. Torassa^a, M. Tosi^{a,b}, M. Zanetti, P. Zotto^{a,b}, A. Zucchetta^{a,b,2}, G. Zumerle^{a,b}

INFN Sezione di Pavia ^a, Università di Pavia ^b, Pavia, Italy

A. Braghieri^a, A. Magnani^a, P. Montagna^{a,b}, S.P. Ratti^{a,b}, V. Re^a, C. Riccardi^{a,b}, P. Salvini^a, I. Vai^a, P. Vitulo^{a,b}

INFN Sezione di Perugia ^a, Università di Perugia ^b, Perugia, Italy

L. Alunni Solestizi^{a,b}, M. Biasini^{a,b}, G.M. Bilei^a, D. Ciangottini^{a,b,2}, L. Fanò^{a,b}, P. Lariccia^{a,b}, G. Mantovani^{a,b}, M. Menichelli^a, A. Saha^a, A. Santocchia^{a,b}, A. Spiezia^{a,b}

INFN Sezione di Pisa ^a, Università di Pisa ^b, Scuola Normale Superiore di Pisa ^c, Pisa, Italy

K. Androsov^{a,27}, P. Azzurri^a, G. Bagliesi^a, J. Bernardini^a, T. Boccali^a, G. Broccolo^{a,c}, R. Castaldi^a, M.A. Ciocci^{a,27}, R. Dell'Orso^a, S. Donato^{a,c,2}, G. Fedi, L. Foà^{a,c†}, A. Giassi^a, M.T. Grippo^{a,27}, F. Ligabue^{a,c}, T. Lomtadze^a, L. Martini^{a,b}, A. Messineo^{a,b}, F. Palla^a, A. Rizzi^{a,b}, A. Savoy-Navarro^{a,28}, A.T. Serban^a, P. Spagnolo^a, P. Squillacioti^{a,27}, R. Tenchini^a, G. Tonelli^{a,b}, A. Venturi^a, P.G. Verdini^a

INFN Sezione di Roma ^a, Università di Roma ^b, Roma, Italy

L. Barone^{a,b}, F. Cavallari^a, G. D'imperio^{a,b,2}, D. Del Re^{a,b}, M. Diemoz^a, S. Gelli^{a,b}, C. Jorda^a, E. Longo^{a,b}, F. Margaroli^{a,b}, P. Meridiani^a, F. Micheli^{a,b}, G. Organtini^{a,b}, R. Paramatti^a, F. Preiato^{a,b}, S. Rahatlou^{a,b}, C. Rovelli^a, F. Santanastasio^{a,b}, P. Traczyk^{a,b,2}

INFN Sezione di Torino ^a, Università di Torino ^b, Torino, Italy, Università del Piemonte Orientale ^c, Novara, Italy

N. Amapane^{a,b}, R. Arcidiacono^{a,c,2}, S. Argiro^{a,b}, M. Arneodo^{a,c}, R. Bellan^{a,b}, C. Biino^a, N. Cartiglia^a, M. Costa^{a,b}, R. Covarelli^{a,b}, A. Degano^{a,b}, N. Demaria^a, L. Finco^{a,b,2}, B. Kiani^{a,b}, C. Mariotti^a, S. Maselli^a, E. Migliore^{a,b}, V. Monaco^{a,b}, E. Monteil^{a,b}, M. Musich^a, M.M. Obertino^{a,b}, L. Pacher^{a,b}, N. Pastrone^a, M. Pelliccioni^a, G.L. Pinna Angioni^{a,b}, F. Ravera^{a,b}, A. Romero^{a,b}, M. Ruspa^{a,c}, R. Sacchi^{a,b}, A. Solano^{a,b}, A. Staiano^a, U. Tamponi^a

INFN Sezione di Trieste ^a, Università di Trieste ^b, Trieste, Italy

S. Belforte^a, V. Candelise^{a,b,2}, M. Casarsa^a, F. Cossutti^a, G. Della Ricca^{a,b}, B. Gobbo^a, C. La Licata^{a,b}, M. Marone^{a,b}, A. Schizzi^{a,b}, T. Umer^{a,b}, A. Zanetti^a

Kangwon National University, Chunchon, Korea

S. Chang, A. Kropivnitskaya, S.K. Nam

Kyungpook National University, Daegu, Korea

D.H. Kim, G.N. Kim, M.S. Kim, D.J. Kong, S. Lee, Y.D. Oh, A. Sakharov, D.C. Son

Chonbuk National University, Jeonju, Korea

J.A. Brochero Cifuentes, H. Kim, T.J. Kim, M.S. Ryu

Chonnam National University, Institute for Universe and Elementary Particles, Kwangju, Korea

S. Song

Korea University, Seoul, Korea

S. Choi, Y. Go, D. Gyun, B. Hong, M. Jo, H. Kim, Y. Kim, B. Lee, K. Lee, K.S. Lee, S. Lee, S.K. Park, Y. Roh

Seoul National University, Seoul, Korea

H.D. Yoo

University of Seoul, Seoul, Korea

M. Choi, H. Kim, J.H. Kim, J.S.H. Lee, I.C. Park, G. Ryu

Sungkyunkwan University, Suwon, Korea

Y. Choi, Y.K. Choi, J. Goh, D. Kim, E. Kwon, J. Lee, I. Yu

Vilnius University, Vilnius, Lithuania

A. Juodagalvis, J. Vaitkus

National Centre for Particle Physics, Universiti Malaya, Kuala Lumpur, Malaysia

I. Ahmed, Z.A. Ibrahim, J.R. Komaragiri, M.A.B. Md Ali²⁹, F. Mohamad Idris³⁰, W.A.T. Wan Abdullah, M.N. Yusli

Centro de Investigacion y de Estudios Avanzados del IPN, Mexico City, Mexico

E. Casimiro Linares, H. Castilla-Valdez, E. De La Cruz-Burelo, I. Heredia-de La Cruz³¹, A. Hernandez-Almada, R. Lopez-Fernandez, A. Sanchez-Hernandez

Universidad Iberoamericana, Mexico City, Mexico

S. Carrillo Moreno, F. Vazquez Valencia

Benemerita Universidad Autonoma de Puebla, Puebla, Mexico

S. Carpinteyro, I. Pedraza, H.A. Salazar Ibarguen

Universidad Autónoma de San Luis Potosí, San Luis Potosí, Mexico

A. Morelos Pineda

University of Auckland, Auckland, New Zealand

D. Krofcheck

University of Canterbury, Christchurch, New Zealand

P.H. Butler, S. Reucroft

National Centre for Physics, Quaid-I-Azam University, Islamabad, Pakistan

A. Ahmad, M. Ahmad, Q. Hassan, H.R. Hoorani, W.A. Khan, T. Khurshid, M. Shoaib

National Centre for Nuclear Research, Swierk, Poland

H. Bialkowska, M. Bluj, B. Boimska, T. Frueboes, M. Górski, M. Kazana, K. Nawrocki, K. Romanowska-Rybinska, M. Szleper, P. Zalewski

Institute of Experimental Physics, Faculty of Physics, University of Warsaw, Warsaw, Poland
G. Brona, K. Bunkowski, K. Doroba, A. Kalinowski, M. Konecki, J. Krolikowski, M. Misiura, M. Olszewski, M. Walczak

Laboratório de Instrumentação e Física Experimental de Partículas, Lisboa, Portugal
P. Bargassa, C. Beirão Da Cruz E Silva, A. Di Francesco, P. Faccioli, P.G. Ferreira Parracho, M. Gallinaro, N. Leonardo, L. Lloret Iglesias, F. Nguyen, J. Rodrigues Antunes, J. Seixas, O. Toldaiev, D. Vadrucio, J. Varela, P. Vischia

Joint Institute for Nuclear Research, Dubna, Russia
S. Afanasiev, P. Bunin, M. Gavrilenko, I. Golutvin, I. Gorbunov, A. Kamenev, V. Karjavin, V. Konoplyanikov, A. Lanev, A. Malakhov, V. Matveev³², P. Moisezenz, V. Palichik, V. Perelygin, S. Shmatov, S. Shulha, N. Skatchkov, V. Smirnov, A. Zarubin

Petersburg Nuclear Physics Institute, Gatchina (St. Petersburg), Russia
V. Golovtsov, Y. Ivanov, V. Kim³³, E. Kuznetsova, P. Levchenko, V. Murzin, V. Oreshkin, I. Smirnov, V. Sulimov, L. Uvarov, S. Vavilov, A. Vorobyev

Institute for Nuclear Research, Moscow, Russia
Yu. Andreev, A. Dermenev, S. Gninenko, N. Golubev, A. Karneyeu, M. Kirsanov, N. Krasnikov, A. Pashenkov, D. Tlisov, A. Toropin

Institute for Theoretical and Experimental Physics, Moscow, Russia
V. Epshteyn, V. Gavrilov, N. Lychkovskaya, V. Popov, I. Pozdnyakov, G. Safronov, A. Spiridonov, E. Vlasov, A. Zhokin

National Research Nuclear University 'Moscow Engineering Physics Institute' (MEPhI), Moscow, Russia
A. Bylinkin

P.N. Lebedev Physical Institute, Moscow, Russia
V. Andreev, M. Azarkin³⁴, I. Dremin³⁴, M. Kirakosyan, A. Leonidov³⁴, G. Mesyats, S.V. Rusakov, A. Vinogradov

Skobeltsyn Institute of Nuclear Physics, Lomonosov Moscow State University, Moscow, Russia
A. Baskakov, A. Belyaev, E. Boos, V. Bunichev, M. Dubinin³⁵, L. Dudko, A. Ershov, A. Gribushin, V. Klyukhin, O. Kodolova, I. Lokhtin, I. Myagkov, S. Obraztsov, S. Petrushanko, V. Savrin

State Research Center of Russian Federation, Institute for High Energy Physics, Protvino, Russia
I. Azhgirey, I. Bayshev, S. Bitioukov, V. Kachanov, A. Kalinin, D. Konstantinov, V. Krychkin, V. Petrov, R. Ryutin, A. Sobol, L. Tourtchanovitch, S. Troshin, N. Tyurin, A. Uzunian, A. Volkov

University of Belgrade, Faculty of Physics and Vinca Institute of Nuclear Sciences, Belgrade, Serbia
P. Adzic³⁶, M. Ekmedzic, J. Milosevic, V. Rekovic

Centro de Investigaciones Energéticas Medioambientales y Tecnológicas (CIEMAT), Madrid, Spain
J. Alcaraz Maestre, E. Calvo, M. Cerrada, M. Chamizo Llatas, N. Colino, B. De La Cruz, A. Delgado Peris, D. Domínguez Vázquez, A. Escalante Del Valle, C. Fernandez Bedoya, J.P. Fernández Ramos, J. Flix, M.C. Fouz, P. Garcia-Abia, O. Gonzalez Lopez, S. Goy Lopez, J.M. Hernandez, M.I. Josa, E. Navarro De Martino, A. Pérez-Calero Yzquierdo, J. Puerta Pelayo, A. Quintario Olmeda, I. Redondo, L. Romero, M.S. Soares

Universidad Autónoma de Madrid, Madrid, Spain

C. Albajar, J.F. de Trocóniz, M. Missiroli, D. Moran

Universidad de Oviedo, Oviedo, Spain

H. Brun, J. Cuevas, J. Fernandez Menendez, S. Folgueras, I. Gonzalez Caballero, E. Palencia Cortezon, J.M. Vizan Garcia

Instituto de Física de Cantabria (IFCA), CSIC-Universidad de Cantabria, Santander, Spain

I.J. Cabrillo, A. Calderon, J.R. Castiñeiras De Saa, P. De Castro Manzano, J. Duarte Campderros, M. Fernandez, G. Gomez, A. Graziano, A. Lopez Virto, J. Marco, R. Marco, C. Martinez Rivero, F. Matorras, F.J. Munoz Sanchez, J. Piedra Gomez, T. Rodrigo, A.Y. Rodríguez-Marrero, A. Ruiz-Jimeno, L. Scodellaro, I. Vila, R. Vilar Cortabitarte

CERN, European Organization for Nuclear Research, Geneva, Switzerland

D. Abbaneo, E. Auffray, G. Auzinger, M. Bachtis, P. Baillon, A.H. Ball, D. Barney, A. Benaglia, J. Bendavid, L. Benhabib, J.F. Benitez, G.M. Berruti, P. Bloch, A. Bocci, A. Bonato, C. Botta, H. Breuker, T. Camporesi, G. Cerminara, S. Colafranceschi³⁷, M. D'Alfonso, D. d'Enterria, A. Dabrowski, V. Daponte, A. David, M. De Gruttola, F. De Guio, A. De Roeck, S. De Visscher, E. Di Marco, M. Dobson, M. Dordevic, B. Dorney, T. du Pree, N. Dupont, A. Elliott-Peisert, G. Franzoni, W. Funk, D. Gigi, K. Gill, D. Giordano, M. Girone, F. Glege, R. Guida, S. Gundacker, M. Guthoff, J. Hammer, P. Harris, J. Hegeman, V. Innocente, P. Janot, H. Kirschenmann, M.J. Kortelainen, K. Kousouris, K. Krajczar, P. Lecoq, C. Lourenço, M.T. Lucchini, N. Magini, L. Malgeri, M. Mannelli, A. Martelli, L. Masetti, F. Meijers, S. Mersi, E. Meschi, F. Moortgat, S. Morovic, M. Mulders, M.V. Nemallapudi, H. Neugebauer, S. Orfanelli³⁸, L. Orsini, L. Pape, E. Perez, A. Petrilli, G. Petrucciani, A. Pfeiffer, D. Piparo, A. Racz, G. Rolandi³⁹, M. Rovere, M. Ruan, H. Sakulin, C. Schäfer, C. Schwick, A. Sharma, P. Silva, M. Simon, P. Sphicas⁴⁰, D. Spiga, J. Steggemann, B. Stieger, M. Stoye, Y. Takahashi, D. Treille, A. Triossi, A. Tsirou, G.I. Veres¹⁸, N. Wardle, H.K. Wöhri, A. Zagozdinska⁴¹, W.D. Zeuner

Paul Scherrer Institut, Villigen, Switzerland

W. Bertl, K. Deiters, W. Erdmann, R. Horisberger, Q. Ingram, H.C. Kaestli, D. Kotlinski, U. Langenegger, D. Renker, T. Rohe

Institute for Particle Physics, ETH Zurich, Zurich, Switzerland

F. Bachmair, L. Bäni, L. Bianchini, M.A. Buchmann, B. Casal, G. Dissertori, M. Dittmar, M. Donegà, M. Dünser, P. Eller, C. Grab, C. Heidegger, D. Hits, J. Hoss, G. Kasieczka, W. Lustermann, B. Mangano, A.C. Marini, M. Marionneau, P. Martinez Ruiz del Arbol, M. Masciovecchio, D. Meister, P. Musella, F. Nessi-Tedaldi, F. Pandolfi, J. Pata, F. Pauss, L. Perrozzi, M. Peruzzi, M. Quittnat, M. Rossini, A. Starodumov⁴², M. Takahashi, V.R. Tavolaro, K. Theofilatos, R. Wallny

Universität Zürich, Zurich, Switzerland

T.K. Aarrestad, C. Amsler⁴³, L. Caminada, M.F. Canelli, V. Chiochia, A. De Cosa, C. Galloni, A. Hinzmann, T. Hreus, B. Kilminster, C. Lange, J. Ngadiuba, D. Pinna, P. Robmann, F.J. Ronga, D. Salerno, Y. Yang

National Central University, Chung-Li, Taiwan

M. Cardaci, K.H. Chen, T.H. Doan, C. Ferro, Sh. Jain, R. Khurana, M. Konyushikhin, C.M. Kuo, W. Lin, Y.J. Lu, R. Volpe, S.S. Yu

National Taiwan University (NTU), Taipei, Taiwan

R. Bartek, P. Chang, Y.H. Chang, Y.W. Chang, Y. Chao, K.F. Chen, P.H. Chen, C. Dietz, F. Fiori,

U. Grundler, W.-S. Hou, Y. Hsiung, Y.F. Liu, R.-S. Lu, M. Miñano Moya, E. Petrakou, J.F. Tsai, Y.M. Tzeng

Chulalongkorn University, Faculty of Science, Department of Physics, Bangkok, Thailand

B. Asavapibhop, K. Kovitangoon, G. Singh, N. Srimanobhas, N. Suwonjandee

Cukurova University, Adana, Turkey

A. Adiguzel, S. Cerci⁴⁴, C. Dozen, S. Girgis, G. Gokbulut, Y. Guler, E. Gurpinar, I. Hos, E.E. Kangal⁴⁵, A. Kayis Topaksu, G. Onengut⁴⁶, K. Ozdemir⁴⁷, S. Ozturk⁴⁸, B. Tali⁴⁴, H. Topakli⁴⁸, M. Vergili, C. Zorbilmez

Middle East Technical University, Physics Department, Ankara, Turkey

I.V. Akin, B. Bilin, S. Bilmis, B. Isildak⁴⁹, G. Karapinar⁵⁰, U.E. Surat, M. Yalvac, M. Zeyrek

Bogazici University, Istanbul, Turkey

E.A. Albayrak⁵¹, E. Gülmez, M. Kaya⁵², O. Kaya⁵³, T. Yetkin⁵⁴

Istanbul Technical University, Istanbul, Turkey

K. Cankocak, S. Sen⁵⁵, F.I. Vardarli

Institute for Scintillation Materials of National Academy of Science of Ukraine, Kharkov, Ukraine

B. Grynyov

National Scientific Center, Kharkov Institute of Physics and Technology, Kharkov, Ukraine

L. Levchuk, P. Sorokin

University of Bristol, Bristol, United Kingdom

R. Aggleton, F. Ball, L. Beck, J.J. Brooke, E. Clement, D. Cussans, H. Flacher, J. Goldstein, M. Grimes, G.P. Heath, H.F. Heath, J. Jacob, L. Kreczko, C. Lucas, Z. Meng, D.M. Newbold⁵⁶, S. Paramesvaran, A. Poll, T. Sakuma, S. Seif El Nasr-storey, S. Senkin, D. Smith, V.J. Smith

Rutherford Appleton Laboratory, Didcot, United Kingdom

K.W. Bell, A. Belyaev⁵⁷, C. Brew, R.M. Brown, D.J.A. Cockerill, J.A. Coughlan, K. Harder, S. Harper, E. Olaiya, D. Petyt, C.H. Shepherd-Themistocleous, A. Thea, L. Thomas, I.R. Tomalin, T. Williams, W.J. Womersley, S.D. Worm

Imperial College, London, United Kingdom

M. Baber, R. Bainbridge, O. Buchmuller, A. Bundock, D. Burton, S. Casasso, M. Citron, D. Colling, L. Corpe, N. Cripps, P. Dauncey, G. Davies, A. De Wit, M. Della Negra, P. Dunne, A. Elwood, W. Ferguson, J. Fulcher, D. Futyan, G. Hall, G. Iles, G. Karapostoli, M. Kenzie, R. Lane, R. Lucas⁵⁶, L. Lyons, A.-M. Magnan, S. Malik, J. Nash, A. Nikitenko⁴², J. Pela, M. Pesaresi, K. Petridis, D.M. Raymond, A. Richards, A. Rose, C. Seez, A. Tapper, K. Uchida, M. Vazquez Acosta⁵⁸, T. Virdee, S.C. Zenz

Brunel University, Uxbridge, United Kingdom

J.E. Cole, P.R. Hobson, A. Khan, P. Kyberd, D. Leggat, D. Leslie, I.D. Reid, P. Symonds, L. Teodorescu, M. Turner

Baylor University, Waco, USA

A. Borzou, K. Call, J. Dittmann, K. Hatakeyama, A. Kasmi, H. Liu, N. Pastika

The University of Alabama, Tuscaloosa, USA

O. Charaf, S.I. Cooper, C. Henderson, P. Rumerio

Boston University, Boston, USA

A. Avetisyan, T. Bose, C. Fantasia, D. Gastler, P. Lawson, D. Rankin, C. Richardson, J. Rohlf, J. St. John, L. Sulak, D. Zou

Brown University, Providence, USA

J. Alimena, E. Berry, S. Bhattacharya, D. Cutts, N. Dhingra, A. Ferapontov, A. Garabedian, U. Heintz, E. Laird, G. Landsberg, Z. Mao, M. Narain, S. Sagir, T. Sinthuprasith

University of California, Davis, Davis, USA

R. Breedon, G. Breto, M. Calderon De La Barca Sanchez, S. Chauhan, M. Chertok, J. Conway, R. Conway, P.T. Cox, R. Erbacher, M. Gardner, W. Ko, R. Lander, M. Mulhearn, D. Pellett, J. Pilot, F. Ricci-Tam, S. Shalhout, J. Smith, M. Squires, D. Stolp, M. Tripathi, S. Wilbur, R. Yohay

University of California, Los Angeles, USA

R. Cousins, P. Everaerts, C. Farrell, J. Hauser, M. Ignatenko, D. Saltzberg, E. Takasugi, V. Valuev, M. Weber

University of California, Riverside, Riverside, USA

K. Burt, R. Clare, J. Ellison, J.W. Gary, G. Hanson, J. Heilman, M. Ivova PANEVA, P. Jandir, E. Kennedy, F. Lacroix, O.R. Long, A. Luthra, M. Malberti, M. Olmedo Negrete, A. Shrinivas, H. Wei, S. Wimpenny

University of California, San Diego, La Jolla, USA

J.G. Branson, G.B. Cerati, S. Cittolin, R.T. D'Agnolo, A. Holzner, R. Kelley, D. Klein, J. Letts, I. Macneill, D. Olivito, S. Padhi, M. Pieri, M. Sani, V. Sharma, S. Simon, M. Tadel, A. Vartak, S. Wasserbaech⁵⁹, C. Welke, F. Würthwein, A. Yagil, G. Zevi Della Porta

University of California, Santa Barbara, Santa Barbara, USA

D. Barge, J. Bradmiller-Feld, C. Campagnari, A. Dishaw, V. Dutta, K. Flowers, M. Franco Sevilla, P. Geffert, C. George, F. Golf, L. Gouskos, J. Gran, J. Incandela, C. Justus, N. Mccoll, S.D. Mullin, J. Richman, D. Stuart, I. Suarez, W. To, C. West, J. Yoo

California Institute of Technology, Pasadena, USA

D. Anderson, A. Apresyan, A. Bornheim, J. Bunn, Y. Chen, J. Duarte, A. Mott, H.B. Newman, C. Pena, M. Pierini, M. Spiropulu, J.R. Vlimant, S. Xie, R.Y. Zhu

Carnegie Mellon University, Pittsburgh, USA

V. Azzolini, A. Calamba, B. Carlson, T. Ferguson, Y. Iiyama, M. Paulini, J. Russ, M. Sun, H. Vogel, I. Vorobiev

University of Colorado Boulder, Boulder, USA

J.P. Cumalat, W.T. Ford, A. Gaz, F. Jensen, A. Johnson, M. Krohn, T. Mulholland, U. Nauenberg, J.G. Smith, K. Stenson, S.R. Wagner

Cornell University, Ithaca, USA

J. Alexander, A. Chatterjee, J. Chaves, J. Chu, S. Dittmer, N. Eggert, N. Mirman, G. Nicolas Kaufman, J.R. Patterson, A. Rinkevicius, A. Ryd, L. Skinnari, L. Soffi, W. Sun, S.M. Tan, W.D. Teo, J. Thom, J. Thompson, J. Tucker, Y. Weng, P. Wittich

Fermi National Accelerator Laboratory, Batavia, USA

S. Abdullin, M. Albrow, J. Anderson, G. Apollinari, L.A.T. Bauerdick, A. Beretvas, J. Berryhill, P.C. Bhat, G. Bolla, K. Burkett, J.N. Butler, H.W.K. Cheung, F. Chlebana, S. Cihangir, V.D. Elvira, I. Fisk, J. Freeman, E. Gottschalk, L. Gray, D. Green, S. Grünendahl, O. Gutsche, J. Hanlon, D. Hare, R.M. Harris, J. Hirschauer, B. Hooberman, Z. Hu, S. Jindariani, M. Johnson, U. Joshi, A.W. Jung, B. Klima, B. Kreis, S. Kwan[†], S. Lammel, J. Linacre, D. Lincoln, R. Lipton,

T. Liu, R. Lopes De Sá, J. Lykken, K. Maeshima, J.M. Marraffino, V.I. Martinez Outschoorn, S. Maruyama, D. Mason, P. McBride, P. Merkel, K. Mishra, S. Mrenna, S. Nahn, C. Newman-Holmes, V. O'Dell, K. Pedro, O. Prokofyev, G. Rakness, E. Sexton-Kennedy, A. Soha, W.J. Spalding, L. Spiegel, L. Taylor, S. Tkaczyk, N.V. Tran, L. Uplegger, E.W. Vaandering, C. Vernieri, M. Verzocchi, R. Vidal, H.A. Weber, A. Whitbeck, F. Yang, H. Yin

University of Florida, Gainesville, USA

D. Acosta, P. Avery, P. Bortignon, D. Bourilkov, A. Carnes, M. Carver, D. Curry, S. Das, G.P. Di Giovanni, R.D. Field, M. Fisher, I.K. Furic, J. Hugon, J. Konigsberg, A. Korytov, J.F. Low, P. Ma, K. Matchev, H. Mei, P. Milenovic⁶⁰, G. Mitselmakher, L. Muniz, D. Rank, R. Rossin, L. Shchutska, M. Snowball, D. Sperka, J. Wang, S. Wang, J. Yelton

Florida International University, Miami, USA

S. Hewamanage, S. Linn, P. Markowitz, G. Martinez, J.L. Rodriguez

Florida State University, Tallahassee, USA

A. Ackert, J.R. Adams, T. Adams, A. Askew, J. Bochenek, B. Diamond, J. Haas, S. Hagopian, V. Hagopian, K.F. Johnson, A. Khatiwada, H. Prosper, V. Veeraraghavan, M. Weinberg

Florida Institute of Technology, Melbourne, USA

V. Bhopatkar, M. Hohlmann, H. Kalakhety, D. Mareskas-palcek, T. Roy, F. Yumiceva

University of Illinois at Chicago (UIC), Chicago, USA

M.R. Adams, L. Apanasevich, D. Berry, R.R. Betts, I. Bucinskaite, R. Cavanaugh, O. Evdokimov, L. Gauthier, C.E. Gerber, D.J. Hofman, P. Kurt, C. O'Brien, I.D. Sandoval Gonzalez, C. Silkworth, P. Turner, N. Varelas, Z. Wu, M. Zakaria

The University of Iowa, Iowa City, USA

B. Bilki⁶¹, W. Clarida, K. Dilsiz, S. Durgut, R.P. Gandrajula, M. Haytmyradov, V. Khristenko, J.-P. Merlo, H. Mermerkaya⁶², A. Mestvirishvili, A. Moeller, J. Nachtman, H. Ogul, Y. Onel, F. Ozok⁵¹, A. Penzo, C. Snyder, P. Tan, E. Tiras, J. Wetzel, K. Yi

Johns Hopkins University, Baltimore, USA

I. Anderson, B.A. Barnett, B. Blumenfeld, D. Fehling, L. Feng, A.V. Gritsan, P. Maksimovic, C. Martin, M. Osherson, J. Roskes, U. Sarica, M. Swartz, M. Xiao, Y. Xin, C. You

The University of Kansas, Lawrence, USA

P. Baringer, A. Bean, G. Benelli, C. Bruner, J. Gray, R.P. Kenny III, D. Majumder, M. Malek, M. Murray, D. Noonan, S. Sanders, R. Stringer, Q. Wang, J.S. Wood

Kansas State University, Manhattan, USA

I. Chakaberia, A. Ivanov, K. Kaadze, S. Khalil, M. Makouski, Y. Maravin, A. Mohammadi, L.K. Saini, N. Skhirtladze, I. Svintradze, S. Toda

Lawrence Livermore National Laboratory, Livermore, USA

D. Lange, F. Rebassoo, D. Wright

University of Maryland, College Park, USA

C. Anelli, A. Baden, O. Baron, A. Belloni, B. Calvert, S.C. Eno, C. Ferraioli, J.A. Gomez, N.J. Hadley, S. Jabeen, R.G. Kellogg, T. Kolberg, J. Kunkle, Y. Lu, A.C. Mignerey, Y.H. Shin, A. Skuja, M.B. Tonjes, S.C. Tonwar

Massachusetts Institute of Technology, Cambridge, USA

A. Apyan, R. Barbieri, A. Baty, K. Bierwagen, S. Brandt, W. Busza, I.A. Cali, Z. Demiragli, L. Di Matteo, G. Gomez Ceballos, M. Goncharov, D. Gulhan, G.M. Innocenti, M. Klute, D. Kovalskyi,

Y.S. Lai, Y.-J. Lee, A. Levin, P.D. Luckey, C. McGinn, C. Mironov, X. Niu, C. Paus, D. Ralph, C. Roland, G. Roland, J. Salfeld-Nebgen, G.S.F. Stephans, K. Sumorok, M. Varma, D. Velicanu, J. Veverka, J. Wang, T.W. Wang, B. Wyslouch, M. Yang, V. Zhukova

University of Minnesota, Minneapolis, USA

B. Dahmes, A. Finkel, A. Gude, P. Hansen, S. Kalafut, S.C. Kao, K. Klapoetke, Y. Kubota, Z. Lesko, J. Mans, S. Nourbakhsh, N. Ruckstuhl, R. Rusack, N. Tambe, J. Turkewitz

University of Mississippi, Oxford, USA

J.G. Acosta, S. Oliveros

University of Nebraska-Lincoln, Lincoln, USA

E. Avdeeva, K. Bloom, S. Bose, D.R. Claes, A. Dominguez, C. Fangmeier, R. Gonzalez Suarez, R. Kamalieddin, J. Keller, D. Knowlton, I. Kravchenko, J. Lazo-Flores, F. Meier, J. Monroy, F. Ratnikov, J.E. Siado, G.R. Snow

State University of New York at Buffalo, Buffalo, USA

M. Alyari, J. Dolen, J. George, A. Godshalk, I. Iashvili, J. Kaisen, A. Kharchilava, A. Kumar, S. Rappoccio

Northeastern University, Boston, USA

G. Alverson, E. Barberis, D. Baumgartel, M. Chasco, A. Hortiangtham, A. Massironi, D.M. Morse, D. Nash, T. Orimoto, R. Teixeira De Lima, D. Trocino, R.-J. Wang, D. Wood, J. Zhang

Northwestern University, Evanston, USA

K.A. Hahn, A. Kubik, N. Mucia, N. Odell, B. Pollack, A. Pozdnyakov, M. Schmitt, S. Stoynev, K. Sung, M. Trovato, M. Velasco, S. Won

University of Notre Dame, Notre Dame, USA

A. Brinkerhoff, N. Dev, M. Hildreth, C. Jessop, D.J. Karmgard, N. Kellams, K. Lannon, S. Lynch, N. Marinelli, F. Meng, C. Mueller, Y. Musienko³², T. Pearson, M. Planer, A. Reinsvold, R. Ruchti, G. Smith, S. Taroni, N. Valls, M. Wayne, M. Wolf, A. Woodard

The Ohio State University, Columbus, USA

L. Antonelli, J. Brinson, B. Bylsma, L.S. Durkin, S. Flowers, A. Hart, C. Hill, R. Hughes, K. Kotov, T.Y. Ling, B. Liu, W. Luo, D. Puigh, M. Rodenburg, B.L. Winer, H.W. Wulsin

Princeton University, Princeton, USA

O. Driga, P. Elmer, J. Hardenbrook, P. Hebda, S.A. Koay, P. Lujan, D. Marlow, T. Medvedeva, M. Mooney, J. Olsen, C. Palmer, P. Piroué, X. Quan, H. Saka, D. Stickland, C. Tully, J.S. Werner, A. Zuranski

University of Puerto Rico, Mayaguez, USA

S. Malik

Purdue University, West Lafayette, USA

V.E. Barnes, D. Benedetti, D. Bortoletto, L. Gutay, M.K. Jha, M. Jones, K. Jung, M. Kress, D.H. Miller, N. Neumeister, F. Primavera, B.C. Radburn-Smith, X. Shi, I. Shipsey, D. Silvers, J. Sun, A. Svyatkovskiy, F. Wang, W. Xie, L. Xu, J. Zablocki

Purdue University Calumet, Hammond, USA

N. Parashar, J. Stupak

Rice University, Houston, USA

A. Adair, B. Akgun, Z. Chen, K.M. Ecklund, F.J.M. Geurts, M. Guilbaud, W. Li, B. Michlin, M. Northup, B.P. Padley, R. Redjimi, J. Roberts, J. Rorie, Z. Tu, J. Zabel

University of Rochester, Rochester, USA

B. Betchart, A. Bodek, P. de Barbaro, R. Demina, Y. Eshaq, T. Ferbel, M. Galanti, A. Garcia-Bellido, P. Goldenzweig, J. Han, A. Harel, O. Hindrichs, A. Khukhunaishvili, G. Petrillo, M. Verzetti

The Rockefeller University, New York, USA

L. Demortier

Rutgers, The State University of New Jersey, Piscataway, USA

S. Arora, A. Barker, J.P. Chou, C. Contreras-Campana, E. Contreras-Campana, D. Duggan, D. Ferencek, Y. Gershtein, R. Gray, E. Halkiadakis, D. Hidas, E. Hughes, S. Kaplan, R. Kunnawalkam Elayavalli, A. Lath, K. Nash, S. Panwalkar, M. Park, S. Salur, S. Schnetzer, D. Sheffield, S. Somalwar, R. Stone, S. Thomas, P. Thomassen, M. Walker

University of Tennessee, Knoxville, USA

M. Foerster, G. Riley, K. Rose, S. Spanier, A. York

Texas A&M University, College Station, USA

O. Bouhali⁶³, A. Castaneda Hernandez, M. Dalchenko, M. De Mattia, A. Delgado, S. Dildick, R. Eusebi, W. Flanagan, J. Gilmore, T. Kamon⁶⁴, V. Krutelyov, R. Montalvo, R. Mueller, I. Osipenkov, Y. Pakhotin, R. Patel, A. Perloff, J. Roe, A. Rose, A. Safonov, A. Tatarinov, K.A. Ulmer²

Texas Tech University, Lubbock, USA

N. Akchurin, C. Cowden, J. Damgov, C. Dragoiu, P.R. Duerdo, J. Faulkner, S. Kunori, K. Lamichhane, S.W. Lee, T. Libeiro, S. Undleeb, I. Volobouev

Vanderbilt University, Nashville, USA

E. Appelt, A.G. Delannoy, S. Greene, A. Gurrola, R. Janjam, W. Johns, C. Maguire, Y. Mao, A. Melo, P. Sheldon, B. Snook, S. Tuo, J. Velkovska, Q. Xu

University of Virginia, Charlottesville, USA

M.W. Arenton, S. Boutle, B. Cox, B. Francis, J. Goodell, R. Hirosky, A. Ledovskoy, H. Li, C. Lin, C. Neu, E. Wolfe, J. Wood, F. Xia

Wayne State University, Detroit, USA

C. Clarke, R. Harr, P.E. Karchin, C. Kottachchi Kankanamge Don, P. Lamichhane, J. Sturdy

University of Wisconsin, Madison, USA

D.A. Belknap, D. Carlsmith, M. Cepeda, A. Christian, S. Dasu, L. Dodd, S. Duric, E. Friis, B. Gomber, R. Hall-Wilton, M. Herndon, A. Hervé, P. Klabbers, A. Lanaro, A. Levine, K. Long, R. Loveless, A. Mohapatra, I. Ojalvo, T. Perry, G.A. Pierro, G. Polese, I. Ross, T. Ruggles, T. Sarangi, A. Savin, A. Sharma, N. Smith, W.H. Smith, D. Taylor, N. Woods

†: Deceased

1: Also at Vienna University of Technology, Vienna, Austria

2: Also at CERN, European Organization for Nuclear Research, Geneva, Switzerland

3: Also at State Key Laboratory of Nuclear Physics and Technology, Peking University, Beijing, China

4: Also at Institut Pluridisciplinaire Hubert Curien, Université de Strasbourg, Université de Haute Alsace Mulhouse, CNRS/IN2P3, Strasbourg, France

-
- 5: Also at National Institute of Chemical Physics and Biophysics, Tallinn, Estonia
 - 6: Also at Skobeltsyn Institute of Nuclear Physics, Lomonosov Moscow State University, Moscow, Russia
 - 7: Also at Universidade Estadual de Campinas, Campinas, Brazil
 - 8: Also at Centre National de la Recherche Scientifique (CNRS) - IN2P3, Paris, France
 - 9: Also at Laboratoire Leprince-Ringuet, Ecole Polytechnique, IN2P3-CNRS, Palaiseau, France
 - 10: Also at Joint Institute for Nuclear Research, Dubna, Russia
 - 11: Now at Ain Shams University, Cairo, Egypt
 - 12: Also at Zewail City of Science and Technology, Zewail, Egypt
 - 13: Now at British University in Egypt, Cairo, Egypt
 - 14: Also at Université de Haute Alsace, Mulhouse, France
 - 15: Also at Tbilisi State University, Tbilisi, Georgia
 - 16: Also at Brandenburg University of Technology, Cottbus, Germany
 - 17: Also at Institute of Nuclear Research ATOMKI, Debrecen, Hungary
 - 18: Also at Eötvös Loránd University, Budapest, Hungary
 - 19: Also at University of Debrecen, Debrecen, Hungary
 - 20: Also at Wigner Research Centre for Physics, Budapest, Hungary
 - 21: Also at University of Visva-Bharati, Santiniketan, India
 - 22: Now at King Abdulaziz University, Jeddah, Saudi Arabia
 - 23: Also at University of Ruhuna, Matara, Sri Lanka
 - 24: Also at Isfahan University of Technology, Isfahan, Iran
 - 25: Also at University of Tehran, Department of Engineering Science, Tehran, Iran
 - 26: Also at Plasma Physics Research Center, Science and Research Branch, Islamic Azad University, Tehran, Iran
 - 27: Also at Università degli Studi di Siena, Siena, Italy
 - 28: Also at Purdue University, West Lafayette, USA
 - 29: Also at International Islamic University of Malaysia, Kuala Lumpur, Malaysia
 - 30: Also at Malaysian Nuclear Agency, MOSTI, Kajang, Malaysia
 - 31: Also at Consejo Nacional de Ciencia y Tecnología, Mexico city, Mexico
 - 32: Also at Institute for Nuclear Research, Moscow, Russia
 - 33: Also at St. Petersburg State Polytechnical University, St. Petersburg, Russia
 - 34: Also at National Research Nuclear University 'Moscow Engineering Physics Institute' (MEPhI), Moscow, Russia
 - 35: Also at California Institute of Technology, Pasadena, USA
 - 36: Also at Faculty of Physics, University of Belgrade, Belgrade, Serbia
 - 37: Also at Facoltà Ingegneria, Università di Roma, Roma, Italy
 - 38: Also at National Technical University of Athens, Athens, Greece
 - 39: Also at Scuola Normale e Sezione dell'INFN, Pisa, Italy
 - 40: Also at University of Athens, Athens, Greece
 - 41: Also at Warsaw University of Technology, Institute of Electronic Systems, Warsaw, Poland
 - 42: Also at Institute for Theoretical and Experimental Physics, Moscow, Russia
 - 43: Also at Albert Einstein Center for Fundamental Physics, Bern, Switzerland
 - 44: Also at Adiyaman University, Adiyaman, Turkey
 - 45: Also at Mersin University, Mersin, Turkey
 - 46: Also at Cag University, Mersin, Turkey
 - 47: Also at Piri Reis University, Istanbul, Turkey
 - 48: Also at Gaziosmanpasa University, Tokat, Turkey
 - 49: Also at Ozyegin University, Istanbul, Turkey
 - 50: Also at Izmir Institute of Technology, Izmir, Turkey

51: Also at Mimar Sinan University, Istanbul, Istanbul, Turkey

52: Also at Marmara University, Istanbul, Turkey

53: Also at Kafkas University, Kars, Turkey

54: Also at Yildiz Technical University, Istanbul, Turkey

55: Also at Hacettepe University, Ankara, Turkey

56: Also at Rutherford Appleton Laboratory, Didcot, United Kingdom

57: Also at School of Physics and Astronomy, University of Southampton, Southampton, United Kingdom

58: Also at Instituto de Astrofísica de Canarias, La Laguna, Spain

59: Also at Utah Valley University, Orem, USA

60: Also at University of Belgrade, Faculty of Physics and Vinca Institute of Nuclear Sciences, Belgrade, Serbia

61: Also at Argonne National Laboratory, Argonne, USA

62: Also at Erzincan University, Erzincan, Turkey

63: Also at Texas A&M University at Qatar, Doha, Qatar

64: Also at Kyungpook National University, Daegu, Korea